

Inflation with vector fields revisited: heavy entropy perturbations and primordial black holes

Chong-Bin Chen

Department of Physics, Kobe University, Kobe 657-8501, Japan

E-mail: chongbin@stu.kobe-u.ac.jp

Abstract. We revisit inflation coupled with vector fields employing kinetic coupling in the comoving gauge. It is known that there is a cumulative effect IN^2 on curvature power spectrum. For a large number of e-foldings N , this contribution is so significant that it could violate observational constraints when the ratio of kinetic energy between vector fields and inflaton I is not extremely small. In this paper, we explore the regime where $I \gg 1$, a realm that has not been extensively explored due to the limitations of perturbative methods. We found that the entropy perturbation becomes heavy in this regime and the cumulative effect decays away on super-horizon scales. Consequently, the power spectrum retains its scale invariance in the decoupling limit. By straightforwardly integrating out the heavy modes near horizon-crossing, we derive a low-energy effective field theory describing a massless adiabatic perturbation with an imaginary speed of sound $c_s^2 = -1/3$. Namely, the inflation with vector fields presents a potential mechanism for generating primordial black holes.

Contents

1	Introduction	1
2	Inflation with vector fields	2
2.1	Background	3
2.2	Quadratic action in comoving gauge	4
2.3	Evolution of the adiabatic mode	6
3	EFT under massive entropy mode	7
3.1	Modified dispersion relation	8
3.2	Integrating out the heavy \mathcal{F}	9
4	Primordial black holes	11
4.1	Board case	12
4.2	Sharp case	13
4.3	PBH formation	17
5	Discussion	20
A	Derivation of the quadratic action	21
B	Growing solution of the adiabatic mode	23
C	Bogoliubov coefficients	24

1 Introduction

Inflationary physics has proven successful in phenomenologically explaining the large-scale structure of our universe. The simplest inflationary model, single-field inflation, predicts nearly scale-invariant, Gaussian, and adiabatic primordial perturbations. These predictions are confirmed by Cosmic Microwave Background (CMB) observations [1–3]. However, the single-field model encounters theoretical challenges. These inflationary models are expected to be effective field theories derived from UV completed theories, such as string theory. Despite the anticipated suppression of higher-dimension irrelevant operators by the UV cutoff, they play a crucial role at the low-energy scale during inflation. The UV sensitivity of inflation gives rise to issues like the η -problem [4, 5] and the super-Planckian problem of a single large field [5–7], disrupting the flatness of the scalar field potential.

The study of introducing extra fields during inflation has attracted attention to evade the issues of single-field inflation. In particular, the study of multi-scalar fields exhibiting strongly non-geodesic motion has been extensively examined in recent years [8–14]. In contrast, our focus is on U(1) gauge fields, commonly known as vector fields, as additional fields during inflation. This choice stems not only from the ubiquity of gauge fields as essential components of the standard model (SM) and beyond but also from their rich phenomenological implications in cosmology [15–19]. The breaking of the conformal coupling between vector fields and gravity is necessary to generate sufficiently strong vector fields [19]. Analogous to the non-geodesic motion of scalar fields, vector fields should exhibit background dynamics

and participate alongside scalar fields in driving inflation. The inflationary phase undergoes a transition to new attractors if the potential is steep enough [20], which is very similar to the hyperbolic inflation [8]. This kind of models was firstly constructed to explain the statistical anisotropy in the CMB [21–24]. The vector field is coupled to gravity through $f^2(\phi)F_{\mu\nu}F^{\mu\nu}$. After suitable choices of $f(\phi)$, the dynamics of background vector fields provides an effective potential for the slow-roll scalar field.

Under this new attractor, the power spectrum of curvature perturbation is sourced by the vector field, yielding an additional contribution

$$\mathcal{P}_\zeta = \mathcal{P}_\zeta^{(0)} [1 + \Theta(\theta)IN^2], \quad (1.1)$$

where $N \equiv \ln(-k\tau_e)$ represents the e-folding number of observed mode elapsed since horizon-crossing and $I = 2\epsilon(\rho_A/V)$ is the fraction kinetic energy of the vector field. For one U(1) vector field, $\Theta(\theta) = 24\sin^2\theta$, where θ is the angle between mode and direction of the vector field [22, 25]. The term IN^2 accountable for the amplitude of statistical anisotropy and should be rigorously constrained by CMB observations to $I < 10^{-7}$ for a sufficiently lengthy inflationary period $N \sim 60$ [22, 25]. The exceedingly small parameter implies the presence of a very small but non-zero vector field, potentially giving rise to fine-tuning challenges [26, 27]. Studies have revealed that employing multiple vector fields can mitigate the anisotropy, eventually converging to an isotropic attractor [24]. For the isotropic configuration of a triad of vector fields, $\Theta(\theta) = 16$, relaxing the constraint on I [28]. However, it still needs to be constrained to $I < 10^{-5}$ due to the tilt of the power spectrum caused by the e-folding number N . This is a cumulative effect, i.e., the curvature is sourced by non-zero vector fields and evolves on super-horizon scales.

However, this does not imply that results for large I are undesirable. If we require vector fields to handle a sufficiently large field displacement, indicating that I is not a small parameter, it appears that the second term in (1.1) becomes significant and violates the adiabatic and scale-invariant initial conditions. However, this result lacks reliability because the perturbative method breaks down in this regime. It has been demonstrated that for $I \gtrsim 0.2$, the calculation by using in-in formalism starts to deviate from the numerical results and it is difficult to track the dynamics near and outside the horizon analytically [29, 30]. Numerical findings indicate that the power spectrum does not actually evolve on super-horizon scales [20, 30]. In this paper, we revisit this dilaton-gauge coupling model in comoving gauge and thoroughly explore the $I \gg 1$ case with the assistance of effective field theory (EFT). We will show, the entropy perturbation is super heavy in this regime and the theory can be described by a low-energy EFT of a massless adiabatic perturbation. IN^2 does not occur in this regime; instead, it is replaced by an exponentially enhanced power spectrum, dependent solely on the parameter I . This enhancement also provides a mechanism for generating primordial black holes.

2 Inflation with vector fields

We are considering the spatially flat Friedmann-Lemaître-Robertson-Walker (FLRW) universe, which is characterized by the scale factor $a(t)$ and the Hubble variable is $H(t) = \dot{a}/a$. The Arnowitt-Deser-Misner(ADM) formalism of the metric is [31]

$$ds^2 = -N^2 dt^2 + q_{ij} (N^i dt + dx^i) (N^j dt + dx^j), \quad (2.1)$$

where N is the lapse function, N^i is the shift vector and g_{ij} is the metric of hypersurface. We consider the model of inflaton and $U(1)$ gauge fields, which is called dilaton-gauge inflation in this paper

$$S = \int d^4x \sqrt{-g} \left[-\frac{1}{2} \partial^\mu \phi \partial_\mu \phi - \frac{1}{4} f_{ab}(\phi) F_{\mu\nu}^a F^{b\mu\nu} \right], \quad (2.2)$$

where f_{ab} is the kinetic coupling and only depends on the inflaton.

2.1 Background

We consider one dilaton field ϕ as inflaton and a triplet of $U(1)$ fields and take an isotropic configuration of background evolution, which can be realized by the choice of $U(1)$ fields as following [32, 33]

$$A_0^a = 0, \quad A_i^a = \mathbb{A} \delta_{ai}, \quad f_{ab} = f^2 \delta_{ab}. \quad (2.3)$$

The identification of the spatial indices and internal indices of the field space allows us to achieve the internal gauge transformation of three $U(1)$ gauge fields by the $O(3)$ rotation of the three spatial dimensions in real space. We mention that the discussion doesn't rely on the number of the $U(1)$ fields. If we have only one $U(1)$ field and kinetic coupling with dilaton, there may be anisotropy left in our universe when the energy density of $U(1)$ gauge field is not so small [22, 25]. Although we will see, the theoretical parameterization of power spectrum is different when this energy density is large enough, we still consider isotropic case so that we can only treat scalar modes at linear order.

Under this configurations the Friedmann equations are given by

$$M_{\text{pl}}^2 H^2 \left(3 - \epsilon_\phi - \frac{3}{2} \epsilon_A \right) = V(\phi), \quad \epsilon = \epsilon_\phi + \epsilon_A, \quad (2.4)$$

where $\epsilon \equiv -\dot{H}/H^2$, $\epsilon_\phi \equiv \dot{\phi}^2/(2M_{\text{pl}}^2 H^2)$ and $\epsilon_A \equiv f^2 \dot{\mathbb{A}}^2/(a^2 M_{\text{pl}}^2 H^2)$. It's also useful to define $\dot{\sigma}^2 \equiv \dot{\phi}^2/2 + f^2 \dot{\mathbb{A}}^2/a^2$ as the ‘‘kinetic’’ energy of the matter fields. Then another gravitational equation can be written as

$$H^2 M_{\text{pl}}^2 \epsilon = \dot{\sigma}^2. \quad (2.5)$$

The equations of motion of the matter fields are

$$\ddot{\phi} + 3H\dot{\phi} + V_\phi - 3f_\phi f \frac{\dot{\mathbb{A}}^2}{a^2} = 0, \quad \ddot{\mathbb{A}} + \left(2\frac{\dot{f}}{f} + H \right) \dot{\mathbb{A}} = 0. \quad (2.6)$$

In this paper we assume that $\dot{\phi} < 0$ and $\dot{\mathbb{A}} > 0$. We also define a useful variable, the ratio of the kinetic energy of $U(1)$ fields and dilaton¹

$$h \equiv \sqrt{\frac{\epsilon_A}{2\epsilon_\phi}}. \quad (2.7)$$

But here the ratio h needn't to be a small parameter. In fact, we will consider the larger $h \gg 1$ on small scales for PBH's production. We will also define the slow-roll parameter $\epsilon_h \equiv \dot{h}/(Hh)$, $\eta_h \equiv \dot{\epsilon}_h/(H\epsilon_h)$, $\eta_\phi \equiv \ddot{\phi}/(H\dot{\phi})$ and $\eta_A \equiv \dot{\epsilon}_A/(H\epsilon_A)$. Taking time derivative on the Friedmann equation one can obtain

$$V_\phi = M_{\text{pl}}^2 H^2 \left(6\epsilon + 2\epsilon_\phi \eta_\phi + \frac{3}{2} \epsilon_A \eta_A - 3\epsilon \epsilon_A \right). \quad (2.8)$$

¹The parameter I in [28] is related to h in our paper as $I \simeq 2h^2$.

Inserting V_ϕ into the equation of motion of ϕ we obtain

$$\frac{f_\phi}{f} M_{\text{pl}} \sqrt{2\epsilon_\phi} = 2 \left(1 + \frac{1}{4} \eta_A - \frac{1}{2} \epsilon \right). \quad (2.9)$$

2.2 Quadratic action in comoving gauge

Thanks to the isotropic background and we will work in the quadratic action and the linear fluctuations of the theory hence the vector and tensor fluctuations are decoupled from scalar ones at linear order. After using the helicity decomposition the scalar parts of the $U(1)$ fields can be written as

$$A_0^a = \partial_a \mathbb{Y}, \quad A_i^a = (\mathbb{A} + \delta\mathbb{A}) \delta_{ai} + \epsilon_{iab} \partial_b \mathbb{U} + \partial_i \partial_a \mathbb{M}. \quad (2.10)$$

We do not distinguish indices a and i here because we identified the spatial rotation symmetry with the internal global $O(3)$ symmetry of the space of the gauge fields. The gauge fields enjoys local $U(1)$ symmetry $A_\mu^a \rightarrow A_\mu^a + \partial_\mu \rho^a$, where ρ^a is a arbitrary function. One can fix the scalar gauge freedom of $U(1)$ fields by $\mathbb{M} = 0$ [20]. The \mathbb{Y} is the constrain d.o.f and we will eliminate it latter after fixing the gauge freedoms of gravity.

The scalar fluctuations of gravity and scalar fields can be written as

$$N = 1 + \alpha, \quad N_i = \partial_i \beta, \quad g_{ij} = a^2(t) e^{2\zeta} \delta_{ij}, \quad \phi = \phi(t) + \delta\phi. \quad (2.11)$$

There are four gauge freedoms of the time and spatial coordinate choice. If we have scalar field, in addition to vector fields we still have one physical d.o.f in the theory. The spatial flat gauge is usually used to study the dilaton-gauge theory. In this gauge, this physical d.o.f is the fluctuation of the scalar field $\delta\phi$. On the other hand, the ‘‘comoving’’ gauge is also used in the two-scalar fields [34, 35]. In this gauge, the adiabatic fluctuation is set to zero. The physical d.o.f are the curvature and entropy fluctuations.

In this paper we adopt the similar comoving gauge for the dilaton-gauge model. The adiabatic fluctuation is given by $Q_\sigma \equiv -\sqrt{2}\dot{\sigma}\delta u$, where δu is the velocity potential given by $\delta T_i^0 \equiv (\rho + p)\partial_i \delta u$. For the isotropic one-form gauge fields, we have $\delta T_i^0 = -\dot{\phi}\partial_i \delta\phi - (2f^2\dot{\mathbb{A}}/a^2)\partial_i \delta\mathbb{A}$ [20]. Here ρ and p are the total energy density and pressure of the system and in our model we have $\rho + p = \dot{\phi}^2 + 2f^2\dot{\mathbb{A}}^2/a^2 = 2\dot{\sigma}^2$. It's useful to define the variable $\delta Q = \sqrt{2}f\delta\mathbb{A}/a$. Then the adiabatic fluctuation is given by

$$Q_\sigma \equiv \frac{\dot{\phi}/\sqrt{2}}{\dot{\sigma}} \delta\phi + \frac{f\dot{\mathbb{A}}/a}{\dot{\sigma}} \delta Q. \quad (2.12)$$

We choose the comoving gauge

$$Q_\sigma = 0. \quad (2.13)$$

This is the unitary gauge in the gauge theory, whose Nambu-Goldstone boson is eaten by the metric, as we will see in the next section. Then we have fixed all gauge freedom of the theory. The d.o.f \mathbb{U} in the vector fields is the magnetic fluctuation and decouple with any other modes in our configuration. It only contribute to the isocurvature fluctuation hence we ignore it in the following discussion. We also define the entropy fluctuations. Defining [28, 36]

$$\cos \vartheta \equiv \frac{\dot{\phi}/\sqrt{2}}{\dot{\sigma}}, \quad \sin \vartheta \equiv \frac{f\dot{\mathbb{A}}/a}{\dot{\sigma}}, \quad (2.14)$$

The adiabatic fluctuation reads $Q_\sigma = \cos \vartheta \delta\phi + \sin \vartheta \delta Q$. This fluctuation follows the direction of the classical “trajectory” of the matter fields. The entropy fluctuation is defined by

$$\mathcal{F} \equiv \cos \vartheta \delta Q - \sin \vartheta \delta\phi, \quad (2.15)$$

which is similar to the entropy fluctuation in the two-scalar fields. But here the entropy fluctuations is not equivalent to the isocurvature one because we still have another contribution \mathbb{U} , which is decoupled with ζ and \mathcal{F} .

After imposing the comoving gauge, the equation of motion of the non-dynamical d.o.f α and \mathbb{Y} can be derived and the solutions read

$$\alpha = \frac{\dot{\zeta}}{H}, \quad (2.16)$$

$$\begin{aligned} \partial^2 \mathbb{Y} = & \dot{\mathbb{A}} \left(\zeta - \frac{\dot{\zeta}}{H} \right) - \frac{a}{\sqrt{2}f} \left(\frac{\mathcal{F}}{\sqrt{1+2h^2}} \right) \\ & - \frac{a}{\sqrt{2}f} \left(H - \frac{\dot{f}}{f} + 4f_\phi \frac{\dot{\mathbb{A}}}{a} h \right) \frac{\mathcal{F}}{\sqrt{1+2h^2}}. \end{aligned} \quad (2.17)$$

The d.o.f β is totally eliminated from the quadratic action when we use the constrain equation of α hence we don't need to write down its specific expression. Then after using the background equations (2.6) and (2.9) to eliminate the V , V_ϕ and f_ϕ , and inserting the constrain equations into the quadratic Lagrangian, we obtain

$$\begin{aligned} \mathcal{L}^{(2)} = & a^3 M_{\text{pl}}^2 \epsilon \left(\dot{\zeta}^2 - \frac{1}{a^2} (\partial\zeta)^2 - m_\sigma^2 \zeta^2 \right) + \frac{a^3}{2} \left(\dot{\mathcal{F}}^2 - \frac{1}{a^2} (\partial\mathcal{F})^2 - m_s^2 \mathcal{F}^2 \right), \\ & - 2a^3 \dot{\sigma} h \left(\mathcal{A} \dot{\zeta} + \mathcal{B} H \zeta \right) \mathcal{F}, \end{aligned} \quad (2.18)$$

where the mass m_σ , m_s and the coupling \mathcal{A} , \mathcal{B} are

$$\begin{aligned} \mathcal{A} = 4, \quad \mathcal{B} = \frac{16h^2}{1+2h^2}, \quad m_\sigma^2 = \frac{16h^2}{1+2h^2} H^2, \\ m_s^2 = \frac{8h^4 - 40h^2 - 4}{1+2h^2} H^2 - \frac{12h^4 - 8h^2 - 2}{1+2h^2} \frac{f_{\phi\phi}}{f} M_{\text{pl}}^2 H^2 \epsilon_\phi, \end{aligned} \quad (2.19)$$

where we have discard slow-roll suppressed terms in the slow-low limit and also assumed $|V_{\phi\phi}|/H^2 \ll 1$. This is the decoupling limit $\epsilon \rightarrow 0$ in the EFT. Then ϵ_ϕ and ϵ_A are also vanishing because they are positive quantities.

We find that the curvature and entropy fluctuations are both massive. The mass term of ζ is only dependent on h . For the mass term of \mathcal{F} , the second term can be regards as the contribution from the curved field space, whose curvature is given by $R_{\text{fs}} = -f_{\phi\phi}/f$. If we assume $h = 0$ initially, where we are in the single-field inflation regime, the entropy mass m_s^2 is still non-vanishing and have large negative contribution if the curvature of field space is negatively large enough. In the slow-roll regime, the second derivative of f in the entropy mass becomes $f_{\phi\phi}/f \simeq f_\phi^2/f^2$. Then using (2.9) the mass square of the entropy fluctuation reads

$$m_s^2 \simeq -\frac{8h^2(3+2h^2)}{1+2h^2} H^2. \quad (2.20)$$

Therefore the entropy fluctuation has imaginary mass. This is similar to the so-called geometrical destabilization [11, 12], which is firstly studied in the multi-scalar inflation and then in the inflation with multiple vector fields [20]. The differences are that the curvature fluctuation ζ is massive and we have an additional coupling $\zeta\mathcal{F}$. Hence we next investigate the mode solutions of this Lagrangian.

2.3 Evolution of the adiabatic mode

We are interested in the super-horizon evolution of the adiabatic mode. We can solve the system from the equations of motion, which is shown in spatially flat gauge in [20]. Here we directly find the solutions from the symmetries of Lagrangian. The quadratic action (2.19) in the long-wavelength limit, where the momentum terms are ignored, can be reduced to

$$\mathcal{L}^{(2)} = a^3 M_{\text{pl}}^2 \epsilon \dot{\zeta}^2 + \frac{a^3}{2} \dot{\mathcal{F}}^2 - \frac{a^3}{2} m_s^2 \left(\mathcal{F} + 2\dot{\sigma} h \frac{\mathcal{A}\dot{\zeta} + \mathcal{B}H\zeta}{m_s^2} \right)^2, \quad (2.21)$$

where we obtained the $\zeta\dot{\zeta}$ term through integral by parts. We see that this Lagrangian is invariant under shift transformation

$$\zeta \rightarrow \zeta + \zeta_0, \quad \mathcal{F} \rightarrow \mathcal{F} - \frac{2\dot{\sigma} h \mathcal{B} H}{m_s^2} \zeta_0. \quad (2.22)$$

This symmetry reveals that ζ and \mathcal{F} have constant solutions obeying

$$\mathcal{F}_0 = -\frac{2\dot{\sigma} h \mathcal{B} H}{m_s^2} \zeta_0. \quad (2.23)$$

These constant solutions exist for any value of h . And it's obvious that these mode solutions are not the correction IN^2 in (1.1). We next explore the Lagrangian for small h .

In the two-scalar case discussed in [37], where all the fields are massless after field-redefinition hence the action has Stückelberg-like symmetry. We find in our case, this symmetry occurs in the leading order of h for small h . To see this, we expand the solutions of adiabatic and entropy perturbations near $h = 0$

$$\zeta = \zeta^{(0)} + \zeta^{(1)} + \dots, \quad \mathcal{F} = \mathcal{F}^{(0)} + \mathcal{F}^{(1)} + \dots \quad (2.24)$$

We see in Lagrangian (2.18), the mass terms are $\mathcal{O}(h^2)$, the \mathcal{A} term is $\mathcal{O}(h)$ and the \mathcal{B} term is $\mathcal{O}(h^3)$. If we only consider super-horizon solutions up to $\mathcal{O}(h)$, the leading-order Lagrangian can be written as

$$\mathcal{L}^{(2)} = \frac{a^3}{2} \left(\sqrt{2\epsilon} M_{\text{pl}} \dot{\zeta} - \sqrt{2\mathcal{A}Hh} \mathcal{F} \right)^2 + \frac{a^3}{2} \dot{\mathcal{F}}^2 + \mathcal{O}(h^2). \quad (2.25)$$

We found at leading order of h , the Lagrangian is invariant under

$$\dot{\zeta} \rightarrow \dot{\zeta} + \dot{\zeta}^{(1)}, \quad \mathcal{F} \rightarrow \mathcal{F} + \frac{\sqrt{\epsilon} M_{\text{pl}}}{\mathcal{A}hH} \dot{\zeta}^{(1)} \quad (2.26)$$

The first order $\dot{\zeta}^{(1)}$ is sourced from zero-th order of entropy perturbations $\mathcal{F}^{(0)}$. This source from entropy modes is a cumulative effect hence is dependent on the e-folding number after horizon-crossing

$$\zeta^{(1)} = \int_{N_c}^{N_e} dN \frac{\mathcal{A}h}{\sqrt{\epsilon} M_{\text{pl}}} \mathcal{F}^{(0)} = \frac{\mathcal{A}hN}{\sqrt{\epsilon} M_{\text{pl}}} \mathcal{F}^{(0)}, \quad (2.27)$$

where N_c is the time of horizon-crossing and $N_k \equiv N_e - N_c$ is the e-folding number elapsed since horizon-crossing. For small h this is a small correction to the adiabatic mode. The zero-th order entropy perturbation is decoupled with the adiabatic one and massless in the slow-roll limit. Hence the zeroth-order power spectrum of entropy perturbation is simple $\mathcal{P}_{\mathcal{F}}^{(0)} = H^2/(4\pi^2)$. Then the leading-order correction to the power spectrum of curvature perturbation can be estimated to

$$\delta\mathcal{P}_{\zeta} \simeq 32h^2N^2 \cdot \frac{H^2}{8\pi^2\epsilon M_{\text{pl}}^2}, \quad (h \ll 1) \quad (2.28)$$

which is consistent with the result calculated through in-in formalism [28]. These correction is proportional to square of e-folding number $N \sim 60$, which is a large number for inflation. Hence for anisotropic configuration of vector fields, there is very strong constrain from CMB on the parameter h . The extreme small h may lead to fine-tuning problem [26, 27]. However, these modes is heavy when h is large enough hence dilute rapidly during inflation. To see this, we next explore the large h case.

3 EFT under massive entropy mode

In the EFT formalism, the physical scalar d.o.f at low-energy scale is the Nambu-Goldstone (NG) boson particle coming from breaking the time translation symmetry $t \rightarrow t + \xi^0$ of the de Sitter space by a clock field $\phi(t)$, i.e., the homogeneous inflaton. One can choose the slice of t that the inflaton has no excitation all the time, i.e. the unitary gauge. In this gauge, the only dynamical scalar d.o.f at low-energy is the scalar part of graviton $g_{ij} = a^2(t)e^{2\zeta}\delta_{ij}$, where the scalar $\zeta(t, \mathbf{x})$ is the spatial curvature of the time slice. The EFT of a single scalar field in the unitary gauge can be written as [38]

$$\mathcal{L}_{\text{EFT}} = \sqrt{-g} \left[\frac{M_{\text{pl}}^2}{2} R + M_{\text{pl}}^2 \dot{H} g^{00} - M_{\text{pl}}^2 (3H^2 + \dot{H}) + \dots \right] + \mathcal{L}_{\text{n-u}}, \quad (3.1)$$

where the dots stand for the higher-order terms of $(1 + g^{00})$ and we have ignored the extrinsic curvature fluctuation $\delta K_{\mu\nu}$. $\mathcal{L}_{\text{n-u}}$ is the non-universal parts and for $\omega^2 \ll M^2 + p^2$ [39]

$$\mathcal{L}_{\text{n-u}} = \sqrt{-g} \sum_{n=2} \frac{M_n^4}{n!} \left[(1 + g^{00}) \frac{M^2}{M^2 - \tilde{\partial}^2} \right]^{n-1} (1 + g^{00}) + \dots, \quad (3.2)$$

where M is the mass of heavy fields and $\tilde{\partial} \equiv \partial/a$. These operators are non-local generally due to the hierarchy between the frequency and momentum when the speed of sound is small $c_s \ll 1$. There exist regime in energy scales that the dispersion is non-linear [39, 40]. If $\omega \sim p$ the momentum is also $p \ll M$ and we can ignore the non-local operators.

In order to transform to the spatial flat gauge $g_{ij} = a^2(t)\delta_{ij}$, one can perform a time diffeomorphisms $t \rightarrow \tilde{t} = t - \pi(t, \mathbf{x})$. Then at linear-order the NG boson is related to the curvature fluctuation as $\zeta = -H\pi$. The time component of the metric transforms as

$$g^{00} = \frac{\partial x^0}{\partial \tilde{x}^\mu} \frac{\partial x^0}{\partial \tilde{x}^\nu} \tilde{g}^{\mu\nu} = (1 + \dot{\pi})^2 \tilde{g}^{00} + 2(1 + \dot{\pi}) \partial_i \pi \tilde{g}^{0i} + \tilde{g}^{ij} \partial_i \pi \partial_j \pi \quad (3.3)$$

In the low-energy scale $\omega \sim p \ll M$, we can write down the action in the re-parameterization of time. Dropping the tildes for simplicity the Lagrangian is given by

$$\begin{aligned} \mathcal{L}_{\text{EFT}} = & \sqrt{-g} \left\{ \frac{M_{\text{pl}}^2}{2} R - M_{\text{pl}}^2 \left[3H^2(t + \pi) + \dot{H}(t + \pi) \right] \right. \\ & + M_{\text{pl}}^2 \dot{H}(t + \pi) \left[(1 + \dot{\pi})^2 g^{00} + 2(1 + \dot{\pi}) \partial_i \pi g^{0i} + \partial^i \pi \partial_i \pi \right] + \\ & \left. + \frac{M_2^4}{2} \left[1 + (1 + \dot{\pi})^2 g^{00} + 2(1 + \dot{\pi}) \partial_i \pi g^{0i} + \partial^i \pi \partial_i \pi \right]^2 + \dots \right\} \end{aligned} \quad (3.4)$$

Expanding the action up to second order of fluctuations, the constrain of the lapse function is solved as $\alpha = \epsilon H \pi$ [41]. In the dilaton-gauge theory, from the quadratic action in the spatial flat gauge (A.1), constrain α is given by $\alpha \propto Q_\sigma$, which means that the unitary gauge is the vanishing adiabatic fluctuation at linear order.

In the decoupling limit, the NG boson is decoupled with gravity and becomes a dynamical scalar mode. For the inflation, this decoupling limit is the slow-roll limit $\epsilon \rightarrow 0$. Then the quadratic Lagrangian of NG boson reduces to

$$\mathcal{L}_{\text{EFT}} = a^3 M_{\text{pl}}^2 H^2 \frac{\epsilon}{c_s^2} \left[\dot{\pi}^2 - \frac{c_s^2}{a^2} (\partial \pi)^2 \right], \quad (3.5)$$

where the speed of sound is defined by

$$\frac{1}{c_s^2} \equiv 1 - \frac{2M_2^4}{M_{\text{pl}}^2 \dot{H}}. \quad (3.6)$$

The modification of the speed of sound is provided by the higher operator M_2 and we will show soon that this can be obtained by integrating out the heavy fluctuation at low energy in the dilaton-gauge model.

3.1 Modified dispersion relation

From the quadratic Lagrangian (2.18) we can write down the linear equations of motion

$$\begin{aligned} \ddot{\zeta} + (3 + \eta) H \dot{\zeta} + \left(\frac{k^2}{a^2} + m_\sigma^2 \right) \zeta &= \frac{1}{a^3 \epsilon} \left(a^3 \frac{\dot{\sigma} h \mathcal{A}}{M_{\text{pl}}^2} \mathcal{F} \right) - \frac{\dot{\sigma} h H \mathcal{B}}{\epsilon M_{\text{pl}}^2} \mathcal{F}, \\ \ddot{\mathcal{F}} + 3H \dot{\mathcal{F}} + \left(\frac{k^2}{a^2} + m_s^2 \right) \mathcal{F} &= -2\dot{\sigma} h \left(\mathcal{A} \dot{\zeta} + \mathcal{B} H \zeta \right). \end{aligned} \quad (3.7)$$

We are interested in the decoupling limit where the nontrivial solution $\zeta = \text{constant}$ is permitted hence we drop out the small slow-roll parameters. Then we have $\mathcal{A} = 4$ and $\mathcal{B} = m_\sigma/H^2$. We regard $\dot{\sigma}$ and h as constants. To find the dispersion relation we study the short-wavelength limit where the Hubble friction terms can be disregarded. We have noted that there is also a mass term for curvature fluctuation. The upper bound of the mass is $m_\sigma^2 \lesssim 8H^2$, i.e., the mass of ζ is at most of the same order as the energy scale of inflation. In the short-wavelength limit the contribution of m_σ term can also be ignored. Then the equations of motion read

$$\begin{aligned} \ddot{\zeta}_c + p^2 \zeta_c &= \sqrt{2} h H \mathcal{A} \dot{\mathcal{F}}, \\ \ddot{\mathcal{F}} + p^2 \mathcal{F} + m_s^2 \mathcal{F} &= -\sqrt{2} h H \mathcal{A} \dot{\zeta}_c, \end{aligned} \quad (3.8)$$

where $p = k/a$ is the physical momentum and $\zeta_c \equiv M_{\text{pl}}\sqrt{2\epsilon}\zeta$ is the canonical variable. The schematic solutions of these equations can be written as [42]

$$\begin{aligned}\zeta_c &= \zeta_+ e^{i\omega_+ t} + \zeta_- e^{i\omega_- t}, \\ \mathcal{F} &= \mathcal{F}_+ e^{i\omega_+ t} + \mathcal{F}_- e^{i\omega_- t},\end{aligned}\tag{3.9}$$

where the two frequencies ω_{\pm} are given by

$$\omega_{\pm}^2 = \frac{m_s^2}{2c_s^2} + p^2 \pm \frac{m_s^2}{2c_s^2} \sqrt{1 + \frac{4(1-c_s^2)p^2}{m_s^2 c_s^{-2}}}\tag{3.10}$$

and the speed of sound is given by

$$\frac{1}{c_s^2} = 1 + \frac{32H^2 h^2}{m_s^2}.\tag{3.11}$$

The modification of the dispersion relation of fluctuations is provided by the interaction with $\dot{\zeta}\mathcal{F}$. The heavy entropy fluctuation implies the hierarchy of the two frequencies $\omega_- \ll \omega_+$, which requires $4(1-c_s^2)p^2 \ll m_s^2 c_s^{-2}$. Hence we have a cut-off scale of EFT (3.5) on momentum p_{UV} and the EFT is only valid below this scale. The UV scale is given by

$$p_{\text{UV}}^2 = \frac{|m_s^2 c_s^{-2}|}{4(1-c_s^2)}.\tag{3.12}$$

In the low energy scales, the two scalar modes, which are corresponded to two frequencies, oscillate coherently and we integrate out the heavy mode to eliminate the high-frequency mode from the dynamics of the curvature fluctuation.

3.2 Integrating out the heavy \mathcal{F}

The fluctuation is heavy for $h \gg 1$ and we also have $|m_s^2| \gg m_\sigma^2$ as we have mentioned before. For positive m_s^2 , the operator from coupling $\dot{\zeta}\mathcal{F}$ would reduce the speed of sound of the fluctuation [42]. However from (2.20) the mass square is negative due to the contribution from kinetic coupling $f(\phi)$. We can ignore the slow-roll suppressed terms and the entropy mass is given by (2.20). Then the speed of sound in this decoupling limit is

$$\frac{1}{c_s^2} = 1 - \frac{4(1+2h^2)}{3+2h^2}.\tag{3.13}$$

The speed of sound $c_s^2 \simeq -1/3$ is imaginary for heavy entropy mass $h \gg 1$. The imaginary speed of sound has been studied in the two-scalar inflation recently [12, 14, 43]. And the entropy mass-square in the two-scalar models is also imaginary hence is tachyonic before the sound horizon crossing $p^2 c_s^2 \sim H^2$. The curvature fluctuation sourced by the entropy fluctuation also experiences transient instability before horizon crossing. After the horizon-crossing, the dynamics of fluctuations are influenced by the background. In other words, the mass term m_σ and the Hubble terms become important outside the horizon.

We have noted that the speed of sound is $|c_s| \sim \mathcal{O}(1)$ for large h hence the non-linear dispersion regime is narrower, and we can directly investigate the linear dispersion regime. In the heavy limit $|m_s^2| \gg \omega^2$ we can expand the operator

$$\frac{1}{m_s^2 - \square} = \frac{1}{m_s^2} + \frac{\square}{m_s^4} + \dots, \quad \text{where } \square \equiv -\frac{\partial^2}{\partial t^2} - 3H\frac{\partial}{\partial t} + \frac{\partial^2}{a^2}.\tag{3.14}$$

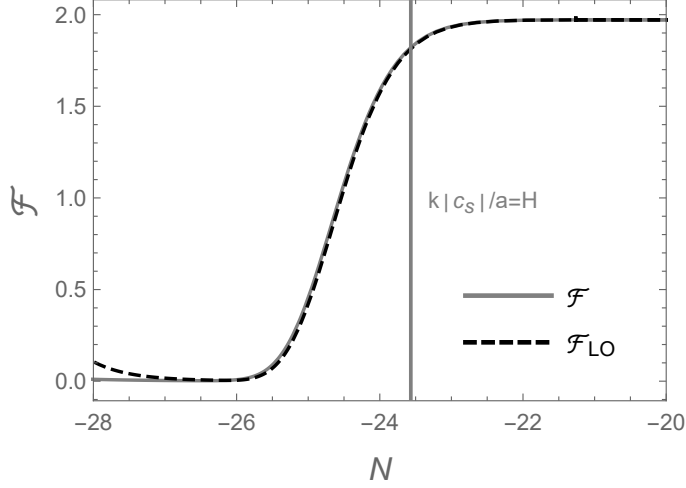


Figure 1. Evolution of entropy perturbation \mathcal{F} for $h = 10$. An instability before horizon-crossing and constant evolution on super-horizon are presented. The scales are arbitrary.

Then the leading-order of the linear equation of motion of \mathcal{F} is given by

$$\mathcal{F}_{\text{LO}} = -\frac{2\dot{\sigma}h(\mathcal{A}\dot{\zeta} + \mathcal{B}H\zeta)}{m_s^2}. \quad (3.15)$$

We show the consistent of the leading-order contribution of \mathcal{F} in Figure 1 for large enough h . The evolution of curvature perturbation on large scales is sourced by non-adiabatic perturbation $\dot{\zeta} = -\delta P_{\text{nad}}H/(\rho + p)$ [44–46]. Then from the leading-order solution of entropy perturbation, the non-adiabatic mode can be represented as

$$\delta P_{\text{nad,LO}} = \frac{m_s^2\dot{\sigma}}{Hh\mathcal{A}}\mathcal{F}_{\text{LO}} + \frac{2\dot{\sigma}^2\mathcal{B}}{\mathcal{A}}\zeta. \quad (3.16)$$

The adiabatic initial condition ensures that the r.h.s. should be relatively small enough on large scales. We can see that the entropy fluctuation doesn't decay outside the horizon, but is proportional to the curvature fluctuation if $\zeta = \text{constant}$ on super-horizon.

We can find that in the EFT of single field, we have only this constant curvature perturbation on large scales. In the slow-roll limit the entropy mass m_s can be calculated by the (2.20). From (3.11) the EFT is only valid under scale

$$p_{\text{UV}} = \frac{3}{4}|m_s|. \quad (3.17)$$

Then after inserting the equation (3.15) into the quadratic action (2.18) we obtain

$$\mathcal{L}_{\text{LO}}^{(2)} = a^3 M_{\text{pl}}^2 \frac{\epsilon}{c_s^2} \left[\dot{\zeta}^2 - \frac{c_s^2}{a^2} (\partial\zeta)^2 \right], \quad (3.18)$$

where c_s is given by (3.13). We have used the integration by parts to eliminate the $\dot{\zeta}\zeta$ terms in the action. Then we found that the mass term of curvature fluctuation is cancelled and ζ is conserved on super-horizon scales.

Different from multi-scalar inflation, where the non-decaying non-adiabatic modes will source to curvature modes so that ζ evolves on super-horizon. In dilation-gauge inflation, we

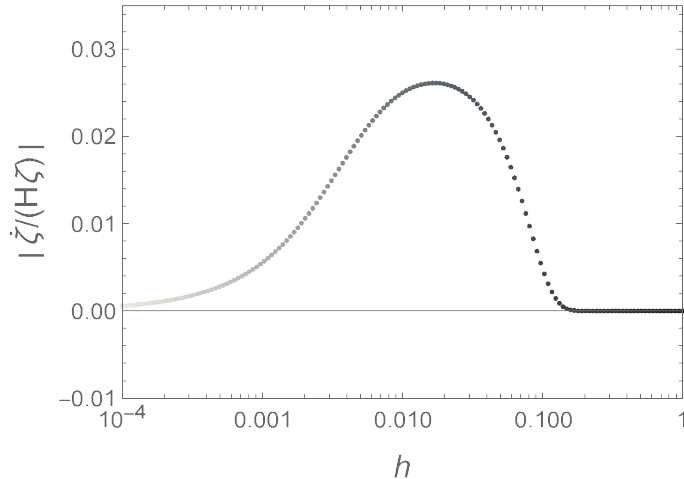


Figure 2. The adiabaticity of super-horizon ($|k\tau_e| = 10^{-15}$) curvature perturbation. As h increases from very small values, the perturbations become non-adiabatic. However, when h exceeds $\mathcal{O}(0.1)$, the perturbation quickly becomes adiabatic.

have constant ζ for non-decaying \mathcal{F} . In other words, \mathcal{F} doesn't play the role of non-adiabatic mode in dilaton-gauge inflation. For mid-value $h \lesssim \mathcal{O}(0.1)$, where $|m_s| \sim H$, the sub-leading terms in δP_{nad} become important and the curvature perturbation evolves on super-horizon. These non-adiabatic contributions are from the cumulative modes (2.27). We show this non-adiabatic occurrence for mild $h \lesssim \mathcal{O}(0.1)$ in Figure 2.

One of the most important findings from this result is that the cumulative modes (2.27) decay away for large h . Because for large h , the modes (3.15) on super-horizon are exactly the constant solutions of the adiabatic mode (2.23). The decaying modes can be also obtained through solving the equation of motion (3.7), which has been studied in spatially flat gauge in [20]. The decaying mode is $\zeta \propto (-k\tau)^{(3-\sqrt{9-96h^2})/2}$. For small h we can expand this solution and find that the leading correction is proportional to e-folding number $\ln(-k\tau) = N$, which is the solution (2.27).

4 Primordial black holes

The remained adiabatic mode experiences an exponential growth before horizon-crossing due to the imaginary speed of sound. Therefore the power spectrum is enhanced exponentially. If vector fields switch on only at late time, the power spectrum is enhanced on small scales so the formations of PBHs in radiation era is possible [47, 48]. And these PBHs can be one of candidates of the dark matter [49–51] and supermassive black holes in our universe [52].

We approach to the PBHs without any specific models ($V(\phi)$ and $f(\phi)$). We here only consider the switch-on of the vector fields at late time N_f during inflation and see the features of power spectrum on small scales for generating PBHs. We choose the horizon-crossing time of the CMB scale $k_{\text{CMB}} = 0.05 \text{Mpc}^{-1}$ as $N_{\text{CMB}} = 0$. Assuming that h has peak at N_f . The curvature modes with different scales that cross the horizon at different time have different contributions to the power spectrum. We can define the corresponding scale

$$k_f|c_s| = a(N_f)H(N_f). \quad (4.1)$$

The modes $k \gg k_f$ that cross the horizon far after the switch-off time experienced nothing hence the power spectrum is the same as the single-field inflation $\mathcal{P}_\zeta^{(0)} = H^2/(8\pi\epsilon M_{\text{pl}}^2)$ on small scales.

On the other hand, the modes $k \ll k_f$ that cross the horizon far before the switch-on time will be impacted by the entropy fluctuation on super-horizon. The entropy fluctuation doesn't decay outside the horizon hence always transfer to the curvature fluctuation. Hence on these large scales, the power spectrum is shifted so different from the single-field one.

The interesting scales are the modes $k \sim k_f$ that cross the horizon near the switch-on time N_f have large enhancements due to the large instability of the entropy fluctuation. Hence we expect that the power spectrum of the curvature fluctuation has exponential enhancements near the scale k_f . We can see from Figure 1 that the mode takes a few e-folding to grow before frozen-in outside the horizon. Hence there are two kinds of power spectrum, the broad ($\delta N \gtrsim \ln(h_0)$) and the sharp ($\delta N \lesssim \ln(h_0)$) switch-on of $h(N)$ [53]. For the shape case, the curvature modes stop growing before crossing the horizon.

4.1 Board case

For this case, we have enough e-folding of $h(N)$ for exponential growth of the modes. The EFT is valid at time N_k satisfying

$$\frac{k}{a(N_v)} = \frac{3}{4}|m_s(N_v)|. \quad (4.2)$$

Then the most contributions to the power spectrum are the modes with $N_v \sim N_f$. We here consider the Gaussian profile of the function

$$h_G(N) = h_0 e^{-(N-N_f)^2/(2\delta N^2)}, \quad (4.3)$$

where the profile is controlled by two parameters $(h_0, \delta N)$. On super-horizon, the entropy modes do not decay and still couple to the curvature ones. Hence we should discuss large-scale modes $k \ll k_f$ and small-scale modes $k \sim k_f$ separately.

Modes with $k \gtrsim k_f$

To characterize the peak of power spectrum with these modes, it's also useful to introduce a dimensionless parameter \mathcal{I} [43, 54]. The quantization of the curvature fluctuation with imaginary speed of sound is quite different from the real one [43]. The difference is that unlike the Bunch-Davies vacuum, the negative frequency modes are non-zero for initial state of EFT due to the different commutation conditions of the mode functions. Taking the super-horizon limit, the leading contribution of the power spectrum is

$$\Delta_\zeta(k) \equiv \frac{\mathcal{P}_\zeta(k)}{\mathcal{P}_\zeta^{(0)}(k)} \simeq e^{2\mathcal{I}(h)}|_{N_k}, \quad (4.4)$$

where the exponential factor is given by (see Appendix B for derivation)

$$\mathcal{I}(h) \simeq \sqrt{2}\pi \left(2 - \sqrt{\frac{1+6h^2}{1+2h^2}} \right) h. \quad (4.5)$$

For modes who start to experiences transient instability earlier, the amplitude will be larger after crossing the horizon. And we need to use a more UV EFT to describe these modes on deeper sub-horizon scales.

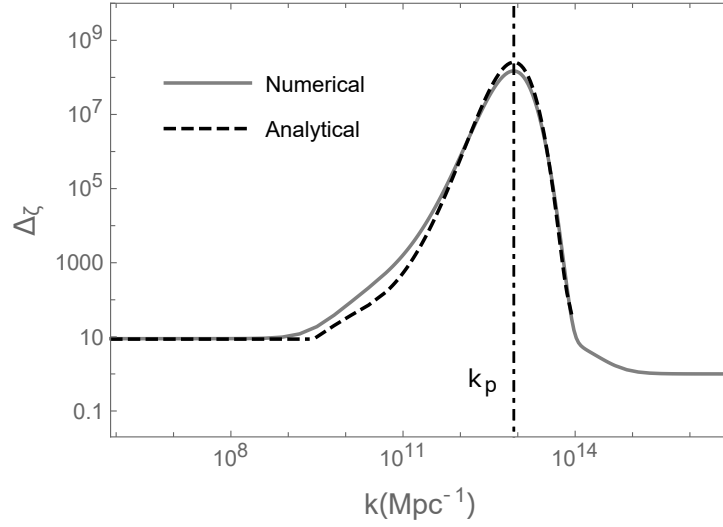


Figure 3. The numerical and analytical results (4.4) of power spectrum for the Gaussian case, where $h_0 = 8$ and $\delta N = 2$.

The scale of peak k_p is the one that has maximal h at time when the modes is growing at N_v , i.e., $N_{pk} = N_v$. Then we have

$$k_p = k_f \cdot \frac{3}{4} \sqrt{\frac{8h_0^2(3 + 2h_0^2)}{1 + 2h_0^2}}. \quad (4.6)$$

We show the numerical and analytical results of our calculation in the Figure 3. One thing we should mention is that (4.4) is not valid for all range of $h(N)$ because the computation is under the vaild of EFT so the mass term of curvature is small compared to the heavy entropy one (or other, large $h(N)$). Hence this estimation work more well for $|m_s^2(N)| \gtrsim 8H^2$ in our Gaussian-profile model.

Modes with $k \ll k_f$

As Figure 3 shown, for the l.h.s of the peak, where the switch occurs after crossing the horizon, the power spectrum is governed by the long range contributions. Hence we can see a shift on the large scale due to the coupling with entropy fluctuation on large scales. We numerically found the amplitude of power spectrum on large scale as the function of h and δN

$$\Delta_\zeta^{(\text{LS})} = (-0.00585h \cdot \delta N + 0.0537h + 0.333\delta N + 1.95)^2. \quad (4.7)$$

The amplitude of large-scale curvature perturbation depends on h and δN linearly and the amplitude of power spectrum $\Delta_\zeta^{(\text{LS})} \gtrsim 10$, i.e., large-scale amplitude is always greater than the one of single-field inflation.

4.2 Sharp case

For very small δN the Gaussian profile can be approximated to a delta function. For analytically computable, we use the top-hat profile

$$h_{\text{TH}} = h_0 [\theta(t - t_1) - \theta(t - t_2)]. \quad (4.8)$$

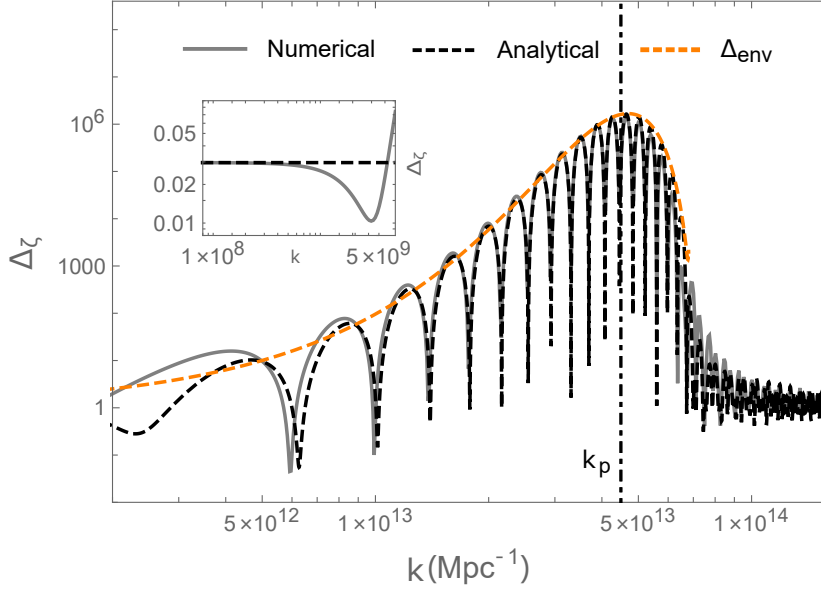


Figure 4. The numerical and analytical results (C.6) of power spectrum for the top-hat case, where $\delta N = 0.4$ and $h_0 = 24$. The envelope (4.14) is shown as orange dashed curve.

The wave number $k_f \simeq H e^{H(t_1+t_2)/2}$ is the scale that the modes cross the horizon during the $h \neq 0$. After the switch-off, the curvature and entropy modes are decoupled. Then the solutions of curvature modes are [55]

$$\begin{aligned} \hat{\zeta}_c(t, \mathbf{k}) = & \left[E_\zeta u_k(t) + F_\zeta u_k^*(t) \right] \hat{a}_\zeta(\mathbf{k}) \\ & + \left[G_\zeta u_k(t) + H_\zeta u_k^*(t) \right] \hat{a}_\mathcal{F}(\mathbf{k}) + \text{h.c.}(-\mathbf{k}), \end{aligned} \quad (4.9)$$

where the annihilation and creation operators of two scalar modes satisfying the commutation relations $[\hat{a}_\alpha(\mathbf{k}), \hat{a}_\beta^\dagger(\mathbf{k}')] = (2\pi)^3 \delta_{\alpha\beta} \delta(\mathbf{k} - \mathbf{k}')$, $[\hat{a}_\alpha^\dagger(\mathbf{k}), \hat{a}_\beta^\dagger(\mathbf{k}')] = [\hat{a}_\alpha(\mathbf{k}), \hat{a}_\beta(\mathbf{k}')] = 0$ and u_k are the mode functions with Bunch-Davies initial conditons

$$u_k(t) = \frac{iH}{\sqrt{2k^3}} \left[1 + ik\tau(t) \right] e^{-ik\tau(t)}. \quad (4.10)$$

Then the power spectrum of curvature perurtbation is given

$$\Delta_\zeta = |E_\zeta - F_\zeta|^2 + |G_\zeta - H_\zeta|^2. \quad (4.11)$$

The non-trivial period is the $h_{\text{TH}} \neq 0$ (which is denoted as region-II), where two kinds of modes strongly couple to each other. We also discuss large-scale modes $k \ll k_f$ and small-scale modes $k \sim k_f$ separately.

Modes with $k \gtrsim k_f$

We simply use the conformal time as the function of t : $\tau(t) = -e^{-Ht}/H$. During t_1 and t_2 with $\delta t \equiv t_2 - t_1 \ll H^{-1}$, one can discard the Hubble friction of the equation of motions. After $t > t_1$, the coupling is switch-on. The duration of $h \neq 0$ is too short $\delta t \ll H^{-1}$ that

we can ignore the evolution of the scale factor. Hence we can ignore the Hubble frictions and curvature mass. Then we can use the equations of motion (3.8) and the WKB-type solutions

$$\begin{aligned}
\hat{\zeta}_c^{\text{II}}(t, \mathbf{k}) &= \sum_{\pm} \left(A_{\pm}^{\zeta} e^{i\omega_{\pm} t} + B_{\pm}^{\zeta} e^{-i\omega_{\pm} t} \right) \hat{a}_{\zeta}(\mathbf{k}) + \left(C_{\pm}^{\zeta} e^{i\omega_{\pm} t} + D_{\pm}^{\zeta} e^{-i\omega_{\pm} t} \right) \hat{a}_{\mathcal{F}}(\mathbf{k}) \\
&\quad + \text{h.c.}(-\mathbf{k}), \\
\hat{\mathcal{F}}^{\text{II}}(t, \mathbf{k}) &= \sum_{\pm} \left(A_{\pm}^{\mathcal{F}} e^{i\omega_{\pm} t} + B_{\pm}^{\mathcal{F}} e^{-i\omega_{\pm} t} \right) \hat{a}_{\zeta}(\mathbf{k}) + \left(C_{\pm}^{\mathcal{F}} e^{i\omega_{\pm} t} + D_{\pm}^{\mathcal{F}} e^{-i\omega_{\pm} t} \right) \hat{a}_{\mathcal{F}}(\mathbf{k}) \\
&\quad + \text{h.c.}(-\mathbf{k}),
\end{aligned} \tag{4.12}$$

where the frequencies are given by (3.10). From the equations of motion, we have relations of the coefficients

$$\begin{aligned}
A_{\pm}^{\mathcal{F}}(C_{\pm}^{\mathcal{F}}) &= i \frac{\omega_{\pm}^2 - p^2}{\sqrt{2} h \mathcal{A} H \omega_{\pm}} A_{\pm}^{\zeta}(C_{\pm}^{\zeta}), \\
B_{\pm}^{\mathcal{F}}(D_{\pm}^{\mathcal{F}}) &= -i \frac{\omega_{\pm}^2 - p^2}{\sqrt{2} h \mathcal{A} H \omega_{\pm}} B_{\pm}^{\zeta}(D_{\pm}^{\zeta}).
\end{aligned}$$

During the short region-II, where the scale factor is nearly invariant, we have $a = a(N_f) = k_f/H$ hence $p = (k/k_f)H$ in the above equations. We have eight unknown coefficients A_{\pm}^{ζ} , B_{\pm}^{ζ} , C_{\pm}^{ζ} and D_{\pm}^{ζ} in the region-II and we have eight boundary conditions at t_1 hence all these coefficients can be completely solved. Then at t_2 we also have eight boundary conditions and the coefficients of (C.3) can be solved to (see Appendix C)

$$\begin{aligned}
E_{\zeta} &\simeq \frac{(S_- + \kappa)^2}{4\kappa S_-} e^{i2\kappa \sinh(\delta N/2) - iS_- \delta N}, \\
F_{\zeta} &\simeq -\frac{S_-^2 - (\kappa + i)^2}{4\kappa} e^{i2\kappa \cosh(\delta N/2)} \cdot i2 \sin(S_- \delta N), \\
G_{\zeta} &\simeq \sqrt{2} h \frac{(\kappa^2 + iS_- + \kappa S_-)(i - \kappa - S_-)}{\kappa S_- S_+^2} e^{i2\kappa \sinh(\delta N/2) - iS_- \delta N}, \\
H_{\zeta} &\simeq \sqrt{2} h \frac{(\kappa^2 + iS_- + \kappa S_-)(i + \kappa - S_-)}{\kappa S_- S_+^2} e^{i2\kappa \cosh(\delta N/2) - iS_- \delta N},
\end{aligned} \tag{4.13}$$

where $\kappa \equiv k/k_f$, $\delta N \equiv H(t_2 - t_1)$ and $S_{\pm} \equiv \omega_{\pm}/H$. We show the agreement between numerical and completed analytical results (see appendix C) in Figure 4. The power spectrum has exponential enhancement near k_f and also rapidly oscillate during these scales. We found E_{ζ} and F_{ζ} are dominated so the power spectrum can be simply written as $\Delta_{\zeta} \simeq \Delta_{\text{env}} \times (\text{rapid oscillation})$, where the envelope is

$$\Delta_{\text{env}} = \left| \frac{e^{-i2S_- \delta N} (\kappa^2 - |S_-|^2)}{4|S_-|^2} \right| \tag{4.14}$$

and the rapid oscillation is characterized by $\text{Exp}(i2\kappa e^{\pm \delta N/2})$, which is only related to the period of non-zero h_{tp} . The enhancement of power spectrum is provided by low-frequency ω_- and period δN together. The scale of peak can be nearly determined by the exponential factor in Δ_{env} , which is estimated by

$$k_p = k_f \cdot \frac{h_0 \sqrt{30 + 104h_0^2 + 56h_0^4}}{2(1 + 2h_0^2)}. \tag{4.15}$$

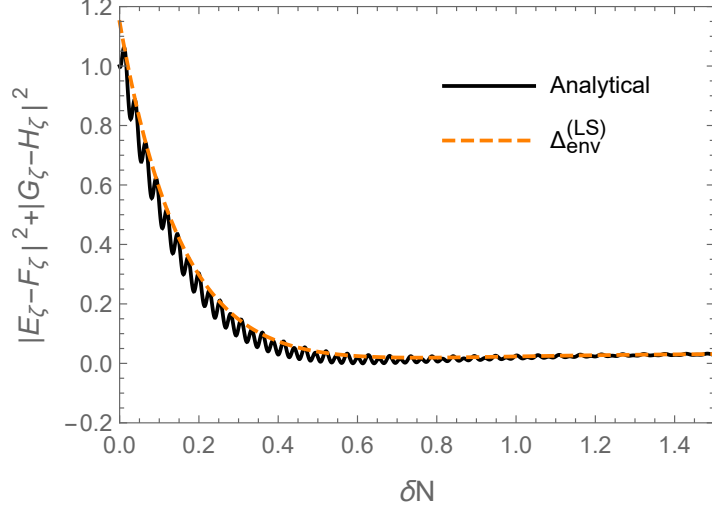


Figure 5. In the top-hat case, the analytical result of large-scale power spectrum as function of δN (4.18), where $h_0 = 24$. The envelope (4.19) is shown as orange dashed curve.

These calculations are only valid near scale $k \gtrsim k_f$ and for $k \ll k_f$ $\Delta_\zeta = 1$, which miss the matching with the numerical results.

Modes with $k \ll k_f$

On large scales, the momentum terms in equations of motion can be ignored and the mass terms and all coupling terms become important. The equations of motion can be solved as

$$\begin{aligned}\hat{\zeta}^{\text{II}}(\tau, \mathbf{k}) &= \sum_{i=\zeta, \mathcal{F}} [c_0^i + c_1^i x^3 + c_+^i x^{1+p_+} + c_-^i x^{1+p_-}] \hat{a}_i(\mathbf{k}) + \text{h.c.}(-\mathbf{k}), \\ \hat{\mathcal{F}}^{\text{II}}(\tau, \mathbf{k}) &= \sum_{i=\zeta, \mathcal{F}} [d_0^i + d_1^i x^3 + d_+^i x^{1+p_+} + d_-^i x^{1+p_-}] \hat{a}_i(\mathbf{k}) + \text{h.c.}(-\mathbf{k}),\end{aligned}\quad (4.16)$$

where $x \equiv -k\tau$ and the coefficients satisfy

$$\begin{aligned}d_0^i &= \frac{2\sqrt{2}h}{3+2h^2} c_0^i, & d_1^i &= -\frac{1}{\sqrt{2}h} c_1^i, \\ d_+^i &= \frac{p_-(1+2h^2)-2}{2\sqrt{2}h(3+4h^2)} c_+^i, & d_-^i &= \frac{p_+(1+2h^2)-2}{2\sqrt{2}h(3+4h^2)} c_-^i.\end{aligned}\quad (4.17)$$

We have eight unknown coefficients c_0^i , c_1^i , c_+^i and c_-^i ($i = \zeta, \mathcal{F}$) in the region-II and eight boundary conditions at t_1 hence all these coefficients can be completely solved. Then at t_2 the coefficients of (C.3) can also be solved². The results are extremely tedious, but we can simple them under some approximations, see appendix C. The results should be real because

²We found that this computation breaks when $x \lesssim 10^{-5}$.

the perturbations become classical on super-horizon. So we can only consider the real parts

$$\begin{aligned}
\text{Re}[E_\zeta] &\simeq \frac{1}{27} [-5 + 32 \cosh(3\delta N)], \\
\text{Re}[F_\zeta] &\simeq \frac{32}{27} \sinh(3\delta N), \\
\text{Re}[G_\zeta] &\simeq \frac{e^{-3\delta N/2}}{3\sqrt{3}} (2e^{3\delta N} + 1) \sin(2\sqrt{6}h\delta N), \\
\text{Re}[H_\zeta] &\simeq \frac{e^{-3\delta N/2}}{3\sqrt{3}} (2e^{3\delta N} - 1) \sin(2\sqrt{6}h\delta N).
\end{aligned} \tag{4.18}$$

We found that, for fixed δN , $|G_\zeta - H_\zeta|$ oscillates around zero when changing h . The oscillation is characterized by $\sin(2\sqrt{6}h\delta N)$ and is not significant on amplitude. This is because, on large scales, the dynamics of curvature perturbation is almost a constant and weakly depends on the frequency. For large h , the dynamics is determined by an EFT of massless curvature perturbation with sound speed $c_s \simeq -1/3$. On the other hand, the amplitudes of $|E_\zeta - F_\zeta|$ and $|G_\zeta - H_\zeta|$ exponentially depend on δN . We can smooth out the oscillation and only estimate the envelope of the power spectrum as

$$\Delta_{\text{env}}^{(\text{LS})} = \frac{1}{729} (25 + 1024e^{-6\delta N} - 212e^{-3\delta N}), \tag{4.19}$$

as Figure 5 shows. We can see $\Delta_\zeta < 1$, in other words, the amplitude of power spectrum on large scales is always smaller than the one of single-field inflation and is not sensitive to h for sharp case. We should mention that this result is also valid for board case with top-hat profile of h . For $\delta N \gg 1$, we have $\Delta_{\text{env}}^{(\text{LS})} \simeq 0.034$, which is not sensitive to δN either.

4.3 PBH formation

After treating the power spectrum on large and small scales for board and sharp case, we can also compare them with the amplitude of the curvature power spectrum required for PBH formation. The fraction of PBHs at formation time can be estimated in a model-independent way [56]

$$\beta_{\text{PBH}} = 3.7 \times 10^{-9} \left(\frac{\gamma}{0.2} \right)^{-1/2} \left(\frac{g_{*,f}}{10.75} \right)^{1/4} \left(\frac{M_{\text{PBH}}}{M_\odot} \right)^{1/2} f_{\text{PBH}}, \tag{4.20}$$

where γ can be calculated analytically as $\gamma = 0.2$ [50], $g_{*,f}$ is the effective number of relativistic degrees of freedom at formation time, M_{PBH} is the mass of PBHs at formation time and $f_{\text{PBH}} \equiv \Omega_{\text{PBH}}/\Omega_{\text{DM}}$ is the present-day fraction of PBH density.

On the other hand, the β can be related to initial conditions of matter power spectrum through collapse theory of Newtonian gravity. The well-used model is the Press-Schechter one [57]. After assuming the Gaussian distribution of overdensity and simply taking the critical density contrast as the threshold $\delta_c = 0.4$ [58], the β can be obtained to

$$\beta_{\text{PBH}} \simeq \frac{\sigma}{\sqrt{2\pi}\delta_c} \text{Exp}\left(-\frac{\delta_c^2}{2\sigma^2}\right), \tag{4.21}$$

where $\sigma^2 \ll \delta_c^2$ is the variance of the distribution. Smaller σ implies less contrast exceeding the critical value, resulting in less β_{PBH} . The variance can be calculated from primordial power spectrum as [59]

$$\sigma^2(R) \simeq \frac{16}{81} \int d\ln q W^2(q, R) (qR)^4 \mathcal{P}_\zeta(q), \tag{4.22}$$

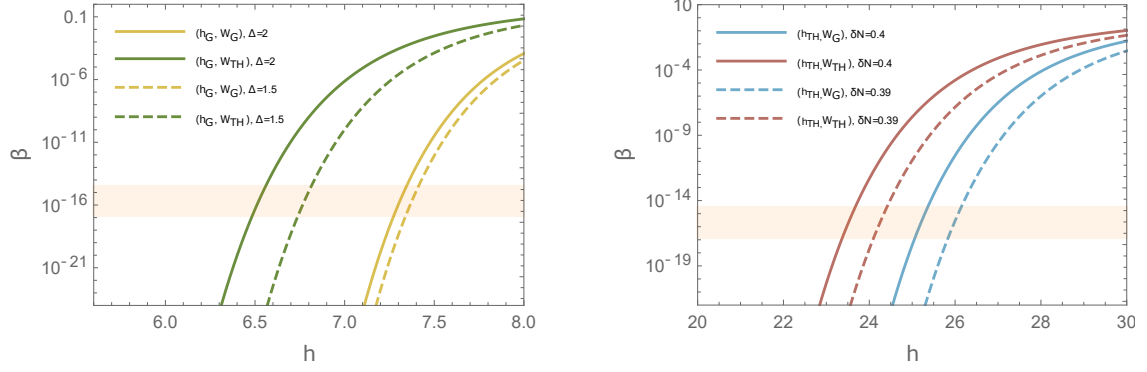


Figure 6. The fraction of PBHs at formation β_{PBH} v.s. height of peaks h . Solid curves denote the cases of $\delta N = 2$ for h_{G} and $\delta N = 0.4$ for h_{TH} , while dashed curves denote the cases of smaller δN . Orange region denotes regime that $f_{\text{PBH}} = 1$ between $10^{-17} M_{\odot} < M_{\text{PBH}} < 10^{-12} M_{\odot}$.

where the window function $W(q, R)$ is selected to Gaussian or top-hat usually and the co-moving horizon size of PBH formed is related to the mass as $R^{-1} = k_p$, where [60]

$$M_{\text{PBH}} = 30 M_{\odot} \left(\frac{\gamma}{0.2} \right) \left(\frac{g_{*,f}}{10.75} \right)^{-1/6} \left(\frac{k_p}{2.9 \times 10^5 \text{Mpc}^{-1}} \right)^{-2}. \quad (4.23)$$

For inflation with a triad of vector fields, where both large-scale and PBH-scale are not trivial, the enhancement at PBH scale comparing with CMB scale is

$$\Delta \mathcal{P}_{\zeta} \equiv \frac{\mathcal{P}_{\zeta}(k_p)}{\mathcal{P}_{\zeta}(k_{\text{CMB}})} = \frac{\Delta_{\zeta}(k_p)}{\Delta_{\zeta}^{(\text{LS})}}. \quad (4.24)$$

The power spectrum at CMB scale is $\mathcal{P}_{\zeta}(k_{\text{CMB}}) = 2 \times 10^{-9}$. For board case this is given by (4.4) and (4.7), while for sharp case, the rapid oscillation will be smoothed out by window function and we can use (4.14) and (4.19).

If we consider the window where the PBHs can be the candidate of dark matter: $10^{-17} M_{\odot} < M_{\text{PBH}} < 10^{-12} M_{\odot}$ and $f_{\text{PBH}} = 1$, from (4.20) we obtain $1.2 \times 10^{-17} < \beta_{\text{PBH}} < 3.7 \times 10^{-15}$. Then from (4.21) the variance for PBH formation in this mass regimes is $0.047 < \sigma < 0.051$. When the power spectrum is peaked at k_p , the variance is reduced to $\sigma^2 \simeq \mathcal{P}_{\zeta}(k_p)/5$. It's seem that we need $\mathcal{P}_{\zeta}(k_p) \sim 10^{-2}$ between $10^{12} \text{Mpc}^{-1} < k_p < 10^{15} \text{Mpc}^{-1}$ to generate sufficient PBHs. However, because the profile of the peak is very sensitive to h and δN and the large-scale power spectrum also depends on these parameters. And the fraction β_{PBH} is exponentially dependent on the power spectrum. Slightly changing profile of the peak will lead to significant change in β_{PBH} . We show how β_{PBH} depend on parameters in Figure 6 for board Gaussian peaks and sharp top-hat peaks. We have used $R = k_p^{-1}$, which are the scales of peaks and can be separately obtained through (4.6) and (4.15) for Gaussian and top-hat examples. The β_{PBH} decays rapidly for smaller parameter, i.e., the smaller height and fatness of the peaks. Also, the difference of using different window functions is also distinguishable.

The mass spectrum of PBHs are shown in Figure 7 for board Gaussian peaks and in Figure 8 for sharp top-hat peaks. We choose the parameters of these examples as following table. For solid curves, we choose the parameters so that the PBHs are responsible for total dark matter $f_{\text{PBH}} = 1$ in our universe. The time of non-vanishing vector fields are chosen

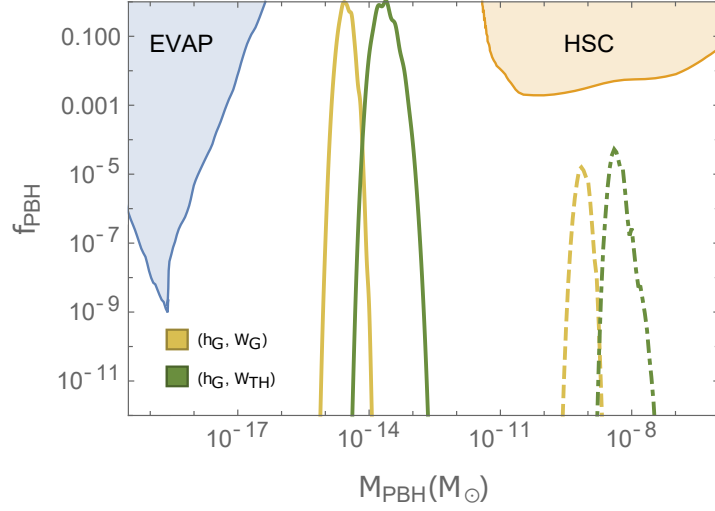


Figure 7. Abundance of PBHs as dark matter for board($\delta N \gtrsim 1$) Gaussian profile of peak h_G .

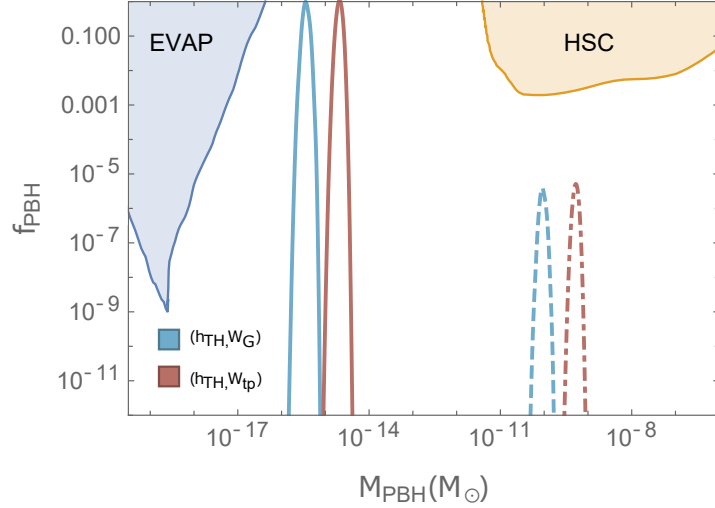


Figure 8. Abundance of PBHs as dark matter for shape($\delta N \lesssim 1$) top-hat profile of peak h_{TH} .

		(h_G, W_G)	(h_G, W_{TH})	(h_{TH}, W_G)	(h_{TH}, W_{TH})
Solid	h	7.258	5.997	24.546	19.285
	δN	2	2	0.4	0.4
Dashed	h	7.200	5.997	24.246	19.285
	δN	2	1.5	0.4	0.395

as $N_f = 31.5$ for all solid examples to avoid constraints from observations of evaporation of PBHs due to Hawking radiation (EVAP) [56] and microlensing of stars in M31 by Subaru Hyper SuprimeCam (HSC) [61]. For dashed curves, we choose different parameters so that $f_{PBH} < 1$ and also different $N_f = 25.3$, which corresponds to larger PBH mass formation. We have seen in Figure 6 the abundance is sensitive to these parameter. As the first and the

third column show, a mere 1% decrease in h leads to a drastic drop in abundance from 1 to 10^{-5} . For top-hat profile of peak h_{TH} , the abundance is also sensitive to δN (4.14). So we can see in the last column of table, 1% decrease in δN also reduces f_{PBH} to 10^{-5} .

We also compare the results of using Gaussian and top-hat window function. The choice of way of smoothing out the fluctuations increases the uncertainty in the results of PBH formation [62, 63]. We demonstrate a significant difference in the parameters required when using different window functions. For example, the first row in table, To generate the same abundance of PBHs, the required h differs by up to 20% when using Gaussian and top-hat window functions. We usually need a larger primordial density in Gaussian smoothing. Furthermore, we also find that using different window functions results in variations in the peak position of f_{PBH} . The mass of formation is usually greater when using top-hat window function. In the examples, this difference reaches up to $M_{\text{peak,TH}}/M_{\text{peak,G}} \sim 10$.

5 Discussion

In this paper we explore the inflation kinetically coupled to vector fields through function $f(\phi)$ in the large h regime. We revisit this model in the comoving gauge, encompassing coupled curvature and entropy perturbations. By directly analyzing the symmetries of the Lagrangian, we identify solutions for these perturbations on super-horizon scales. We find that, in addition to the solution contributing to the IN^2 correction due to the Stückelberg-like symmetry when h is very small, there exists constant solutions (2.23) for the system at any value of h . However, when h is large, the entropy perturbation has significant and imaginary mass (2.20). In this regime, the leading-order solution of the entropy perturbation on super-horizon scales is given by the constant solution (2.23). This implies that the solution contributing to the IN^2 correction quickly decays on super-horizon scales, leaving only the constant solution. This maintains a scale-invariant power spectrum. In the effective field theory (3.18), the curvature perturbation is massless and has an imaginary speed of sound, leading to an exponential enhancement before crossing the horizon. This is similar to the case of hyperbolic inflation, but the difference lies in the fact that outside the horizon, entropy perturbations do not decay and remain strongly coupled to curvature perturbations, resulting in the large-scale modes also depending on the details of the dynamics of vector fields.

In addition to driving inflation, the enhancement of the power spectrum can also serve as a mechanism for the generation of primordial black holes (PBHs). This requires a strong excitation of the vector field during the late stages of inflation. We discussed two toy examples of h : Gaussian and top-hat. The Gaussian is employed to discuss the broad case, while the top-hat is used to address the sharp case, as both yield more precise analytical results. Due to the non-decaying entropy perturbations, the large-scale power spectrum is shifted compared to the single-field one. The amplitude of the shift depends on the details of vector fields dynamics, i.e., δN and h , as shown in (4.7) and (4.19). For the shape top-hat case, this amplitude is only a function of δN , allowing for an analytical calculation of the shape of the power spectrum. Given the exponential dependence of the power spectrum shape on these parameters and the subsequent exponential dependence of PBH abundance on the power spectrum shape, the PBH abundance is highly sensitive to these parameters. Whether it's h or δN , even slight variations can significantly reduce the abundance of PBHs. Certainly, this sensitivity is also related to the specific details of the PBH collapse. For instance, we demonstrated that under the same δ_c , smoothing the same fluctuations in different ways can lead to vastly different results, not only in PBH abundance but also in the masses of PBH

formation. For example, compared to a Gaussian window function, using a top-hat window function typically results in PBHs with smaller masses. Further investigation is required to address this question comprehensively.

Now, we delve into another regime, characterized by a relatively large energy of the vector field. In this scenario, the contributions to inflationary predictions differ significantly from the case where h is very small. Many questions need to be reconsidered in this regime, such as the anisotropy for one vector field and non-Gaussianity. We posit that the discussions in this paper are also applicable to a single vector field. In this case, the IN^2 term in power spectrum, which served as a contribution to anisotropy for small h case, is replaced by other constant modes. It is imperative for us to calculate the anisotropy in this regime. Additionally, when considering a charged field as the inflaton, whether the perturbative Schwinger effect from the electric field is crucial to inflationary predictions is also a question that warrants consideration. Regarding PBHs, we are discussing the isotropic configuration of vector fields as an example. Although it bears similarities to hyperbolic inflation, in general, vector fields themselves exhibit phenomenology distinct from scalar fields, such as anisotropy for a single vector field and chirality for symmetry breaking. These differences manifest in the generated PBHs and induced gravitational waves. We intend to present these studies in the near future.

Acknowledgments

I would like to thank Jiro Soda for helpful discussions. C-B.C. was supported by Japanese Government (MEXT) Scholarship and China Scholarship Council (CSC).

A Derivation of the quadratic action

In this appendix we show the full quadratic action of the inflation with a triad of vector fields. We will fix the gauge freedoms of gravity as comoving gauge and then eliminate the non-dynamical degrees of freedom.

We can write down the Lagrangian of gravity, scalar field and $U(1)$ fields as following

$$\begin{aligned}\mathcal{L}_g &= N\sqrt{q} \left[\frac{M_{\text{pl}}^2}{2} \left({}^{(3)}R + K_{ij}K^{ij} - K^2 \right) \right], \\ \mathcal{L}_\phi &= \sqrt{q} \left[\frac{1}{2N} \pi^2 - \frac{N}{2} \partial_i \phi \partial^i \phi - NV(\phi) \right], \\ \mathcal{L}_A &= \sqrt{q} \left[\frac{f_{ab}}{2N} q^{ik} (E_i^a + F_{ij}^a N^j) (E_k^b + F_{kl}^b N^l) - \frac{N f_{ab}}{4} q^{ik} q^{jl} F_{ij}^a F_{kl}^b \right],\end{aligned}$$

where we have defined $\pi = \dot{\phi} - N^j \phi_{|j}$ and q_{ij} is the induced metric of space-like hypersurface and $E_i^a \equiv F_{0i}^a$. The extrinsic curvature and the spatial curvature are

$$\begin{aligned}K_{ij} &= \frac{1}{2N} (\dot{q}_{ij} - 2N_{(i|j)}), \\ {}^{(3)}R &= \left(q_{ij,kl} + q_{mn} {}^{(3)}\Gamma_{ij}^m {}^{(3)}\Gamma_{kl}^n \right) (q^{ik} q^{jl} - q^{ij} q^{kl})\end{aligned}$$

The quadratic action is given by

$$\begin{aligned}
\mathcal{L}^{(2)} = \frac{a^3}{2} \Bigg\{ & \left[-6M_{\text{pl}}^2 H^2 \alpha + \dot{\phi}^2 \alpha - 2V_\phi \delta\phi - 2\dot{\phi}\delta\dot{\phi} + 3f^2 \frac{\dot{\mathbb{A}}^2}{a^2} \alpha - 6ff_\phi \frac{\dot{\mathbb{A}}^2}{a^2} \delta\phi \right. \\
& - \sqrt{2}f \frac{\dot{\mathbb{A}}}{a} \left(3\delta\dot{Q} + 3\left(H - \frac{\dot{f}}{f}\right)\delta Q \right) + 2f^2 \frac{\dot{\mathbb{A}}}{a^2} \partial^2 \mathbb{Y} \Big] \alpha + \frac{2}{a^2} \left(\dot{\phi}\delta\phi - 2M_{\text{pl}}^2 H A \right. \\
& + \sqrt{2}f \frac{\dot{\mathbb{A}}}{a} \delta Q \Big) \partial^2 \beta + (\delta\dot{\phi})^2 - \frac{1}{a^2} (\partial_i \delta\phi)^2 - V_{\phi\phi} (\delta\phi)^2 + \frac{3}{2} \left[(\delta\dot{Q})^2 \right. \\
& + 2\left(H - \frac{\dot{f}}{f}\right)\delta Q \delta\dot{Q} + \left(H - \frac{\dot{f}}{f}\right)^2 (\delta Q)^2 \Big] - \frac{1}{a^2} (\partial_i \delta Q)^2 + \frac{f^2}{a^2} \partial^2 \mathbb{Y} \partial^2 \mathbb{Y} \\
& - \sqrt{2} \frac{f}{a} \left(\delta\dot{Q} + \left(H - \frac{\dot{f}}{f}\right)\delta Q \right) \partial^2 \mathbb{Y} + 2\sqrt{2}a^2 f_\phi \frac{\dot{\mathbb{A}}}{a} \left[3\delta\dot{Q} + 3\left(H - \frac{\dot{f}}{f}\right)\delta Q \right] \\
& \left. - 4ff_\phi \frac{\dot{\mathbb{A}}}{a^2} \partial^2 \mathbb{Y} \delta\phi + \frac{3}{a^2} (f_\phi^2 + ff_{\phi\phi}) \mathbb{A}^2 (\delta\phi)^2 \right. \\
& + \left[\left(12H\dot{\zeta} - \frac{4}{a^2} \partial^2 \zeta \right) M_{\text{pl}}^2 + 6f^2 \frac{\dot{\mathbb{A}}^2}{a^2} \zeta \right] A + 4M_{\text{pl}}^2 \frac{1}{a^2} \dot{\zeta} \partial^2 \beta \\
& - \left(6\dot{\zeta}^2 + 36\dot{\zeta}\zeta + 54h^2 \zeta^2 + \frac{2}{a^2} \zeta \partial^2 \zeta \right) M_{\text{pl}}^2 + 6\zeta \left[\dot{\phi} - V_\phi \delta\phi + ff_\phi \frac{\dot{\mathbb{A}}^2}{a^2} \delta\phi \right. \\
& \left. \left. + \sqrt{2}f \frac{\dot{\mathbb{A}}}{2a} \left(\delta\dot{Q} + \left(H - \frac{\dot{f}}{f}\right)\delta Q \right) - f^2 \frac{\dot{\mathbb{A}}}{3a^2} \partial^2 \mathbb{Y} + 3\zeta^2 \left(3\dot{\phi}^2 + 5f^2 \frac{\dot{\mathbb{A}}^2}{a^2} \right) \right] \right\}, \tag{A.1}
\end{aligned}$$

$$\begin{aligned}
& + \left[\left(12H\dot{\zeta} - \frac{4}{a^2} \partial^2 \zeta \right) M_{\text{pl}}^2 + 6f^2 \frac{\dot{\mathbb{A}}^2}{a^2} \zeta \right] A + 4M_{\text{pl}}^2 \frac{1}{a^2} \dot{\zeta} \partial^2 \beta \\
& - \left(6\dot{\zeta}^2 + 36\dot{\zeta}\zeta + 54h^2 \zeta^2 + \frac{2}{a^2} \zeta \partial^2 \zeta \right) M_{\text{pl}}^2 + 6\zeta \left[\dot{\phi} - V_\phi \delta\phi + ff_\phi \frac{\dot{\mathbb{A}}^2}{a^2} \delta\phi \right. \\
& \left. + \sqrt{2}f \frac{\dot{\mathbb{A}}}{2a} \left(\delta\dot{Q} + \left(H - \frac{\dot{f}}{f}\right)\delta Q \right) - f^2 \frac{\dot{\mathbb{A}}}{3a^2} \partial^2 \mathbb{Y} + 3\zeta^2 \left(3\dot{\phi}^2 + 5f^2 \frac{\dot{\mathbb{A}}^2}{a^2} \right) \right] \Bigg\}, \tag{A.2}
\end{aligned}$$

where (A.1) is the parts which do not contain curvature perturbation ζ while (A.2) do. After imposing the comoving gauge (2.13), we can eliminate the inflaton perturbation $\delta\phi$. Then the equations of motion of non-dynamical degrees of freedom α , β and \mathbb{Y} are

$$\begin{aligned}
\alpha &= \frac{\dot{\zeta}}{H}, \quad \partial^2 \mathbb{Y} = \dot{\mathbb{A}} \left(\zeta - \frac{\dot{\zeta}}{H} \right) + \frac{a}{\sqrt{2}f} \left[\delta\dot{Q} + \left(H - \frac{\dot{f}}{f} + 4f_\phi \frac{\dot{\mathbb{A}}}{a} h \right) \delta Q \right], \\
\frac{4}{a^2} M_{\text{pl}}^2 H \partial^2 \beta &= -4M_{\text{pl}}^2 H^2 \left(3 - \epsilon_\phi - \frac{3}{2} \epsilon_A \right) \alpha - M_{\text{pl}} H^2 \left[-12\sqrt{2} \frac{f_\phi}{f} M_{\text{pl}} \epsilon_A h \right. \\
& \quad + 2\sqrt{2} \sqrt{2\epsilon_\phi} (3 + \eta_\phi) h + 3\sqrt{2\epsilon_A} \left(1 - \frac{\dot{f}}{fH} \right) \Big] \delta Q \\
& \quad + M_{\text{pl}} H \sqrt{2\epsilon_A} \left(-\delta\dot{Q} + 2H\eta_h \delta Q + \sqrt{2} \frac{f}{a} \partial^2 \mathbb{Y} \right) \\
& \quad + M_{\text{pl}}^2 \left(12H\dot{\zeta} - \frac{4}{a^2} \partial^2 \zeta \right) + 6M_{\text{pl}}^2 H^2 \epsilon_A \zeta. \tag{A.3}
\end{aligned}$$

After inserting these solutions into the quadratic action and imposing a series of tedious integral by parts, the quadratic action can be written as (2.18), where the mass m_σ , m_s and the coupling \mathcal{A} , \mathcal{B} are

$$\begin{aligned}
\mathcal{A} &= 4 + \mathcal{O}(\epsilon), \quad \mathcal{B} = \frac{16h^2}{1 + 2h^2} + \mathcal{O}(\epsilon), \quad m_\sigma^2 = \frac{16h^2}{1 + 2h^2} H^2, \\
m_s^2 &= \frac{8h^4 - 40h^2 - 4}{1 + 2h^2} H^2 - \frac{12h^4 - 8h^2 - 2}{1 + 2h^2} \frac{f_{\phi\phi}}{f} M_{\text{pl}}^2 H^2 \epsilon_\phi + \frac{2h^2}{1 + 2h^2} V_{\phi\phi} + \mathcal{O}(\epsilon). \tag{A.4}
\end{aligned}$$

All coefficients except m_σ have slow-roll corrections $\mathcal{O}(\epsilon)$. Here ϵ denotes all kinds of slow-roll parameter, i.e., ϵ , ϵ_ϕ , ϵ_A and their higher derivative of time. We consider decoupling limit in this paper hence these corrections can be discarded. Also, we assume the slow-roll condition that $V_{\phi\phi} \ll H^2$ hence the third term in m_s^2 also can be ignored.

B Growing solution of the adiabatic mode

The negative mass square of entropy fluctuation may lead to a imaginary low frequency ω_- . Then the curvature fluctuation start to exponentially grow at some time \tilde{N}_k , which is determined by $\omega_-(\tilde{N}_k) = 0$: $p^2(\tilde{N}_k) = -m_s^2$. If we neglect the slow rolling, the power spectrum is scale invariant on large scales and we can rescale it as $p/H = e^{-N}$. The growing solution of the curvature fluctuation can be written as [54]

$$\zeta \propto \exp \left[\int_{-\ln(|m_s|/H)}^N \frac{|\omega_-|}{H} dN \right], \quad (\text{B.1})$$

where ω_- is given by (3.10)

$$\frac{|\omega_-|}{H} = \sqrt{-\mu^2 - \frac{1}{2}u + \frac{1}{2}\sqrt{u^2 + 128h^2\mu^2}} \quad (\text{B.2})$$

and $\mu \equiv p/H$ and $u \equiv m_s^2/H^2 + 32h^2$. It's useful to define the variable y as $u^2y^2 = u^2 + 128h^2\mu^2$ Then the integration in (B.1) becomes

$$\mathcal{I}(N) \equiv \frac{u}{8\sqrt{2}h} \int_{y_1}^{y_2} \sqrt{b(y-1) - (y^2-1)} \frac{ydy}{y^2-1} \quad (\text{B.3})$$

where the parameter $b \equiv 64h^2/u$, $c \equiv \lambda/u$ and the limits are

$$y_1 = \sqrt{1 + \frac{128h^2\mu^2}{u^2}}, \quad y_2 = \sqrt{1 + \frac{128h^2|m_s|^2}{u^2H^2}}. \quad (\text{B.4})$$

The primitive function above can be calculated and given by

$$F(y) = \frac{u}{8\sqrt{2}h} \left\{ \sqrt{1-b+by-y^2} - \frac{b}{2} \arctan \left[\frac{b-2y}{2\sqrt{1-b+by-y^2}} \right] - \frac{\sqrt{2b}}{2} \arctan \left[\frac{2(1-y) + b(y-1-2)}{2\sqrt{2b}\sqrt{1-b+by-y^2}} \right] \right\}, \quad (\text{B.5})$$

For two $\arctan x$ in $F(y)$ at y_2 , the first one is negative $-\pi/2$ while the second one is positive $\pi/2$ due to $b-2y_2 < 0$ and $2(1-y_2) + b(y_2-1-2) > 0$. On the other hand, the modes will be frozen-in when crossing the horizon hence we take the upper limit at $k|c_s| = aH$, i.e.,

$$y_1 = \sqrt{1 + \frac{128h^2}{u^2|c_s|^2}} \quad (\text{B.6})$$

Summarizing the above computation, we finally have

$$\mathcal{I} = \frac{u}{8\sqrt{2}h} \left\{ -\sqrt{1-b+by_1-y_1^2} + \frac{b}{2} \left[\frac{\pi}{2} + \arctan \left[\frac{b-2y_1}{2\sqrt{1-b+by_1-y_1^2}} \right] \right] - \frac{\sqrt{2b}}{2} \left[\frac{\pi}{2} - \arctan \left[\frac{2(1-y_1) + b(y_1-3)}{2\sqrt{2b}\sqrt{1-b+by_1-y_1^2}} \right] \right] \right\}. \quad (\text{B.7})$$

We can simply take the super-horizon limit $\mu \rightarrow 0$ and in the slow-roll limit,

$$u^2 \simeq \frac{8h^2(1+6h^2)}{1+2h^2}, \quad b \simeq \frac{8(1+2h^2)}{1+6h^2}, \quad y_1 \simeq 1. \quad (\text{B.8})$$

Then the function \mathcal{I} can be reduced to a simply form

$$\mathcal{I}_{\text{approx}} = \sqrt{2\pi} \left(2 - \sqrt{\frac{1+6h^2}{1+2h^2}} \right) h. \quad (\text{B.9})$$

For large $h \gg 1$ we found $\mathcal{I}_{\text{approx}} \simeq 1.186h$, which is very closed to the numerical result $1.193h$ we have found in [20]. We found that the approximation result is good enough for $h \gtrsim 5$.

C Bogoliubov coefficients

For the shape case, we use the top-hat profile of the $h(N)$ for analytical computations,

$$h(N) = h_0 [\theta(t - t_1) - \theta(t - t_2)]. \quad (\text{C.1})$$

Before t_1 , where we denote as region-I, the curvature and entropy modes are decoupled. Hence the solutions are simply the mode function with Bunch-Davies initial conditions, as the same as the single-field case,

$$\begin{aligned} \hat{\zeta}_c^{\text{I}}(t, \mathbf{k}) &= u_k(t) \hat{a}_\zeta(\mathbf{k}) + \text{h.c.}(-\mathbf{k}), \\ \hat{\mathcal{F}}^{\text{I}}(t, \mathbf{k}) &= u_k(t) \hat{a}_\mathcal{F}(\mathbf{k}) + \text{h.c.}(-\mathbf{k}), \end{aligned} \quad (\text{C.2})$$

where u_k is given by (4.10).

After $t > t_1$, which is denoted as region-II, these two scalar fields are coupled to each other hence their modes are also mixed with each other. The governing equations of motion are given by (3.7). We discuss two different non-trivial momentum regimes: near PBHs peak $k \sim k_f$ and large scales $k \ll k_f$, respectively. In order to preserve the continuity of the commutation relations, we should impose the boundary conditions at $t = t_1$ as

$$\begin{aligned} \hat{\zeta}_c^{\text{I}}(t_1^-) &= \hat{\zeta}_c^{\text{II}}(t_1^+), & \dot{\hat{\zeta}}_c^{\text{I}}(t_1^-) &= D_t \hat{\zeta}_c^{\text{II}}(t_1^+), \\ \hat{\mathcal{F}}^{\text{I}}(t_1^-) &= \hat{\mathcal{F}}^{\text{II}}(t_1^+), & \dot{\hat{\mathcal{F}}}^{\text{I}}(t_1^-) &= \dot{\hat{\mathcal{F}}}^{\text{II}}(t_1^+), \end{aligned} \quad (\text{C.3})$$

where $D_t \hat{\zeta}_c \equiv \dot{\hat{\zeta}}_c - \sqrt{2}h\mathcal{A}H\hat{\mathcal{F}}$.

During region-III $t > t_2$, where the curvature and entropy modes are decoupled again, the mode functions are again the ones with Bunch-David vacuum but mixing these two scalar modes,

$$\begin{aligned} \hat{\zeta}_c^{\text{III}}(t, \mathbf{k}) &= \left[E_\zeta u_k(t) + F_\zeta u_k^*(t) \right] \hat{a}_\zeta(\mathbf{k}) + \left[G_\zeta u_k(t) + H_\zeta u_k^*(t) \right] \hat{a}_\mathcal{F}(\mathbf{k}) \\ &\quad + \text{h.c.}(-\mathbf{k}), \\ \hat{\mathcal{F}}^{\text{III}}(t, \mathbf{k}) &= \left[E_\mathcal{F} u_k(t) + F_\mathcal{F} u_k^*(t) \right] \hat{a}_\zeta(\mathbf{k}) + \left[G_\mathcal{F} u_k(t) + H_\mathcal{F} u_k^*(t) \right] \hat{a}_\mathcal{F}(\mathbf{k}) \\ &\quad + \text{h.c.}(-\mathbf{k}). \end{aligned} \quad (\text{C.4})$$

We then also impose the boundary conditions at $t = t_2$ as

$$\begin{aligned}\hat{\zeta}_c^{\text{II}}(t_2^-) &= \hat{\zeta}_c^{\text{III}}(t_2^+), & D_t \hat{\zeta}_c^{\text{II}}(t_2^-) &= \dot{\hat{\zeta}}_c^{\text{III}}(t_2^+), \\ \hat{\mathcal{F}}^{\text{II}}(t_2^-) &= \hat{\mathcal{F}}^{\text{III}}(t_2^+), & \dot{\hat{\mathcal{F}}}^{\text{II}}(t_2^-) &= \dot{\hat{\mathcal{F}}}^{\text{III}}(t_2^+).\end{aligned}\tag{C.5}$$

We have eight coefficients E_i , F_i , G_i and H_i , where $i = \zeta, \mathcal{F}$ and can be determined by the eight boundary conditions at t_2 .

For modes with $k \gtrsim k_f$, the coefficients of curvature perturbations are solved to

$$\begin{aligned}E_\zeta &= \frac{e^{i2\kappa \sinh(\frac{\delta N}{2})}}{4\kappa(S_+^2 - S_-^2)} \sum_{\pm} \pm \frac{S_{\mp}^2 - \kappa^2}{S_{\pm}} \left\{ e^{iS_{\pm}\delta N} [1 + (S_{\pm} - \kappa)^2] - e^{-iS_{\pm}\delta N} [1 + (S_{\pm} + \kappa)^2] \right\}, \\ F_\zeta &= \frac{e^{i2\kappa \cosh(\frac{\delta N}{2})}}{2\kappa(S_+^2 - S_-^2)} \sum_{\pm} \pm \frac{i \sin(S_{\pm}\delta N)}{S_{\pm}} (S_{\mp}^2 - \kappa^2) [S_{\pm}^2 + (1 - \kappa^2 - i2\kappa)], \\ G_\zeta &= \frac{i\sqrt{2}h\mathcal{A}e^{i2\kappa \sinh(\frac{\delta N}{2})}}{4\kappa(S_+^2 - S_-^2)} \sum_{\pm} \pm \frac{1}{S_{\pm}} \left\{ e^{iS_{\pm}\delta N} [\kappa^2 - S_{\pm}(i + \kappa)] (i - \kappa + S_{\pm}) \right. \\ &\quad \left. - e^{-iS_{\pm}\delta N} [\kappa^2 + S_{\pm}(i + \kappa)] (i - \kappa - S_{\pm}) \right\}, \\ H_\zeta &= \frac{i\sqrt{2}h\mathcal{A}e^{i2\kappa \cosh(\frac{\delta N}{2})}}{4\kappa(S_+^2 - S_-^2)} \sum_{\pm} \pm \frac{1}{S_{\pm}} \left\{ e^{iS_{\pm}\delta N} [\kappa^2 - S_{\pm}(i + \kappa)] (i + \kappa + S_{\pm}) \right. \\ &\quad \left. - e^{-iS_{\pm}\delta N} [\kappa^2 + S_{\pm}(i + \kappa)] (i + \kappa - S_{\pm}) \right\},\end{aligned}\tag{C.6}$$

where $\kappa \equiv k/k_f$, $\delta N \equiv H(t_2 - t_1)$ and $S_{\pm} \equiv \omega_{\pm}/H$.

For modes with $k \ll k_f$, the coefficients can be also solved. The final results depends on h , δN and $x_2 = -k\tau_2$ and are extremely tedious. This is because the matching on boundaries is not exact. However we can simple the results under some approximations. Firstly, we are interested in the large h case and we can expand the results as small $1/h$. Secondly, we are considering the super-horizon limit hence $x_2 \ll 1$. Then we can also expand the results as small x_2 . The dominated terms up to first term in small h and first two terms in small x_2 in these two expansions are

$$\begin{aligned}E_\zeta &= \frac{1}{27} [32 \cosh(3\delta N) - 5] + i \frac{4(1 - e^{-3\delta N})}{9x_2^3} + i \frac{e^{-\delta N/2}}{3x_2} \left[\sinh\left(\frac{\delta N}{2}\right) \right. \\ &\quad \left. + 4 \sinh\left(\frac{5\delta N}{2}\right) \right] + \dots, \\ F_\zeta &= \frac{32}{27} \sinh(3\delta N) + i \frac{4(1 - e^{-3\delta N})}{9x_2^3} + i \frac{e^{-\delta N/2}}{3x_2} \left[\sinh\left(\frac{\delta N}{2}\right) + 4 \sinh\left(\frac{5\delta N}{2}\right) \right] + \dots, \\ G_\zeta &= \frac{e^{-3\delta N/2}}{3\sqrt{3}} \left(2e^{3\delta N} + 1 - i \frac{6}{x_2^3} - ie^{2\delta N} \frac{3}{x_2} \right) \sin(2\sqrt{6}h\delta N) + \dots, \\ H_\zeta &= \frac{e^{-3\delta N/2}}{3\sqrt{3}} \left(2e^{3\delta N} - 1 - i \frac{6}{x_2^3} - ie^{2\delta N} \frac{3}{x_2} \right) \sin(2\sqrt{6}h\delta N) + \dots.\end{aligned}\tag{C.7}$$

We find that although the results are complex and the imaginary parts are the functions of x_2 , in $(E_\zeta - F_\zeta)$ and $(G_\zeta - H_\zeta)$, the imaginary parts will be killed to each other. Because perturbations ζ becomes classical and is a constant after horizon-crossing.

References

- [1] G. F. Smoot *et al.*, “Structure in the COBE Differential Microwave Radiometer First-Year Maps”, *Astrophys. J.* **396**, L1 (1992)
- [2] D. N. Spergel *et al.* [WMAP], “First year Wilkinson Microwave Anisotropy Probe (WMAP) observations: Determination of cosmological parameters,” *Astrophys. J. Suppl.* **148**, 175-194 (2003) doi:10.1086/377226 [arXiv:astro-ph/0302209 [astro-ph]].
- [3] N. Aghanim *et al.* [Planck], “Planck 2018 results. VI. Cosmological parameters,” *Astron. Astrophys.* **641**, A6 (2020) [erratum: *Astron. Astrophys.* **652**, C4 (2021)] doi:10.1051/0004-6361/201833910 [arXiv:1807.06209 [astro-ph.CO]].
- [4] E. J. Copeland, A. R. Liddle, D. H. Lyth, E. D. Stewart and D. Wands, “False vacuum inflation with Einstein gravity,” *Phys. Rev. D* **49**, 6410-6433 (1994) doi:10.1103/PhysRevD.49.6410 [arXiv:astro-ph/9401011 [astro-ph]].
- [5] D. Baumann and L. McAllister, “Inflation and String Theory,” Cambridge University Press, 2015, ISBN 978-1-107-08969-3, 978-1-316-23718-2 doi:10.1017/CBO9781316105733 [arXiv:1404.2601 [hep-th]].
- [6] D. H. Lyth, “What would we learn by detecting a gravitational wave signal in the cosmic microwave background anisotropy?,” *Phys. Rev. Lett.* **78**, 1861-1863 (1997) doi:10.1103/PhysRevLett.78.1861 [arXiv:hep-ph/9606387 [hep-ph]].
- [7] D. Baumann and D. Green, “A Field Range Bound for General Single-Field Inflation,” *JCAP* **05**, 017 (2012) doi:10.1088/1475-7516/2012/05/017 [arXiv:1111.3040 [hep-th]].
- [8] A. R. Brown, “Hyperbolic Inflation,” *Phys. Rev. Lett.* **121**, no.25, 251601 (2018) doi:10.1103/PhysRevLett.121.251601 [arXiv:1705.03023 [hep-th]].
- [9] S. Mizuno and S. Mukohyama, “Primordial perturbations from inflation with a hyperbolic field-space,” *Phys. Rev. D* **96**, no.10, 103533 (2017) doi:10.1103/PhysRevD.96.103533 [arXiv:1707.05125 [hep-th]].
- [10] P. Christodoulidis, D. Roest and E. I. Sfakianakis, “Angular inflation in multi-field α -attractors,” *JCAP* **11**, 002 (2019) doi:10.1088/1475-7516/2019/11/002 [arXiv:1803.09841 [hep-th]].
- [11] S. Renaux-Petel and K. Turzyński, “Geometrical Destabilization of Inflation,” *Phys. Rev. Lett.* **117**, no.14, 141301 (2016) doi:10.1103/PhysRevLett.117.141301 [arXiv:1510.01281 [astro-ph.CO]].
- [12] S. Garcia-Saenz, S. Renaux-Petel and J. Ronayne, “Primordial fluctuations and non-Gaussianities in sidetracked inflation,” *JCAP* **07**, 057 (2018) doi:10.1088/1475-7516/2018/07/057 [arXiv:1804.11279 [astro-ph.CO]].
- [13] T. Bjorkmo, “Rapid-Turn Inflationary Attractors,” *Phys. Rev. Lett.* **122**, no.25, 251301 (2019) doi:10.1103/PhysRevLett.122.251301 [arXiv:1902.10529 [hep-th]].
- [14] J. Fumagalli, S. Garcia-Saenz, L. Pinol, S. Renaux-Petel and J. Ronayne, “Hyper-Non-Gaussianities in Inflation with Strongly Nongeodesic Motion,” *Phys. Rev. Lett.* **123**, no.20, 201302 (2019) doi:10.1103/PhysRevLett.123.201302 [arXiv:1902.03221 [hep-th]].
- [15] Y. Akrami *et al.* [Planck], “Planck 2018 results. X. Constraints on inflation,” *Astron. Astrophys.* **641**, A10 (2020) doi:10.1051/0004-6361/201833887 [arXiv:1807.06211 [astro-ph.CO]].

- [16] F. Tavecchio, et al., “The intergalactic magnetic field constrained by Fermi/Large Area Telescope observations of the TeV blazar 1ES 0229+ 200,” *Mon. Not. R. Astron. Soc.* **406**, L70 (2010).
- [17] A. Neronov and I. Vovk, “Evidence for strong extragalactic magnetic fields from Fermi observations of TeV blazars,” *Science* **328**, 73 (2010).
- [18] F. Tavecchio, G. Ghisellini, G. Bonnoli and L. Foschini, “Extreme TeV blazars and the intergalactic magnetic field,” *Mon. Not. R. Astron. Soc.* **414**, 3566 (2011).
- [19] K. Subramanian, “The origin, evolution and signatures of primordial magnetic fields,” *Rept. Prog. Phys.* **79**, no.7, 076901 (2016) doi:10.1088/0034-4885/79/7/076901 [arXiv:1504.02311 [astro-ph.CO]].
- [20] C. B. Chen and J. Soda, “Geometric structure of multi-form-field isotropic inflation and primordial fluctuations,” *JCAP* **05**, no.05, 029 (2022) doi:10.1088/1475-7516/2022/05/029 [arXiv:2201.03160 [hep-th]].
- [21] M. a. Watanabe, S. Kanno and J. Soda, “Inflationary Universe with Anisotropic Hair,” *Phys. Rev. Lett.* **102**, 191302 (2009) doi:10.1103/PhysRevLett.102.191302 [arXiv:0902.2833 [hep-th]].
- [22] M. a. Watanabe, S. Kanno and J. Soda, “The Nature of Primordial Fluctuations from Anisotropic Inflation,” *Prog. Theor. Phys.* **123**, 1041-1068 (2010) doi:10.1143/PTP.123.1041 [arXiv:1003.0056 [astro-ph.CO]].
- [23] S. Kanno, J. Soda and M. a. Watanabe, “Anisotropic Power-law Inflation,” *JCAP* **12**, 024 (2010) doi:10.1088/1475-7516/2010/12/024 [arXiv:1010.5307 [hep-th]].
- [24] K. Yamamoto, M. a. Watanabe and J. Soda, “Inflation with Multi-Vector-Hair: The Fate of Anisotropy,” *Class. Quant. Grav.* **29**, 145008 (2012) doi:10.1088/0264-9381/29/14/145008 [arXiv:1201.5309 [hep-th]].
- [25] N. Bartolo, S. Matarrese, M. Peloso and A. Ricciardone, “Anisotropic power spectrum and bispectrum in the $f(\phi)F^2$ mechanism,” *Phys. Rev. D* **87**, no.2, 023504 (2013) doi:10.1103/PhysRevD.87.023504 [arXiv:1210.3257 [astro-ph.CO]].
- [26] A. Naruko, E. Komatsu and M. Yamaguchi, “Anisotropic inflation reexamined: upper bound on broken rotational invariance during inflation,” *JCAP* **04**, 045 (2015) doi:10.1088/1475-7516/2015/04/045 [arXiv:1411.5489 [astro-ph.CO]].
- [27] T. Fujita and I. Obata, “Does anisotropic inflation produce a small statistical anisotropy?,” *JCAP* **01**, 049 (2018) doi:10.1088/1475-7516/2018/01/049 [arXiv:1711.11539 [astro-ph.CO]].
- [28] M. A. Gorji, S. A. Hosseini Mansoori and H. Firouzjahi, “Inflation with multiple vector fields and non-Gaussianities,” *JCAP* **11**, 041 (2020) doi:10.1088/1475-7516/2020/11/041 [arXiv:2008.08195 [astro-ph.CO]].
- [29] K. Yamamoto, “Primordial Fluctuations from Inflation with a Triad of Background Gauge Fields,” *Phys. Rev. D* **85**, 123504 (2012) doi:10.1103/PhysRevD.85.123504 [arXiv:1203.1071 [astro-ph.CO]].
- [30] H. Funakoshi and K. Yamamoto, “Primordial bispectrum from inflation with background gauge fields,” *Class. Quant. Grav.* **30**, 135002 (2013) doi:10.1088/0264-9381/30/13/135002 [arXiv:1212.2615 [astro-ph.CO]].
- [31] R. L. Arnowitt, S. Deser and C. W. Misner, “The Dynamics of general relativity,” *Gen. Rel. Grav.* **40**, 1997-2027 (2008) doi:10.1007/s10714-008-0661-1 [arXiv:gr-qc/0405109 [gr-qc]].
- [32] A. Maleknejad and M. M. Sheikh-Jabbari, “Non-Abelian Gauge Field Inflation,” *Phys. Rev. D* **84**, 043515 (2011) doi:10.1103/PhysRevD.84.043515 [arXiv:1102.1932 [hep-ph]].
- [33] A. Maleknejad and M. M. Sheikh-Jabbari, “Gauge-flation: Inflation From Non-Abelian Gauge

- Fields,” *Phys. Lett. B* **723**, 224-228 (2013) doi:10.1016/j.physletb.2013.05.001 [arXiv:1102.1513 [hep-ph]].
- [34] A. Achúcarro, J. O. Gong, S. Hardeman, G. A. Palma and S. P. Patil, “Effective theories of single field inflation when heavy fields matter,” *JHEP* **05**, 066 (2012) doi:10.1007/JHEP05(2012)066 [arXiv:1201.6342 [hep-th]].
 - [35] S. Garcia-Saenz, L. Pinol and S. Renaux-Petel, “Revisiting non-Gaussianity in multifield inflation with curved field space,” *JHEP* **01**, 073 (2020) doi:10.1007/JHEP01(2020)073 [arXiv:1907.10403 [hep-th]].
 - [36] H. Firouzjahi, M. A. Gorji, S. A. Hosseini Mansoori, A. Karami and T. Rostami, “Charged Vector Inflation,” *Phys. Rev. D* **100**, no.4, 043530 (2019) doi:10.1103/PhysRevD.100.043530 [arXiv:1812.07464 [hep-th]].
 - [37] A. Achúcarro, V. Atal, C. Germani and G. A. Palma, “Cumulative effects in inflation with ultra-light entropy modes,” *JCAP* **02**, 013 (2017) doi:10.1088/1475-7516/2017/02/013 [arXiv:1607.08609 [astro-ph.CO]].
 - [38] C. Cheung, P. Creminelli, A. L. Fitzpatrick, J. Kaplan and L. Senatore, “The Effective Field Theory of Inflation,” *JHEP* **03**, 014 (2008) doi:10.1088/1126-6708/2008/03/014 [arXiv:0709.0293 [hep-th]].
 - [39] R. Gwyn, G. A. Palma, M. Sakellariadou and S. Syksas, “Effective field theory of weakly coupled inflationary models,” *JCAP* **04**, 004 (2013) doi:10.1088/1475-7516/2013/04/004 [arXiv:1210.3020 [hep-th]].
 - [40] D. Baumann and D. Green, “Equilateral Non-Gaussianity and New Physics on the Horizon,” *JCAP* **09**, 014 (2011) doi:10.1088/1475-7516/2011/09/014 [arXiv:1102.5343 [hep-th]].
 - [41] J. M. Maldacena, “Non-Gaussian features of primordial fluctuations in single field inflationary models,” *JHEP* **05**, 013 (2003) doi:10.1088/1126-6708/2003/05/013 [arXiv:astro-ph/0210603 [astro-ph]].
 - [42] A. Achúcarro, V. Atal, S. Cespedes, J. O. Gong, G. A. Palma and S. P. Patil, “Heavy fields, reduced speeds of sound and decoupling during inflation,” *Phys. Rev. D* **86**, 121301 (2012) doi:10.1103/PhysRevD.86.121301 [arXiv:1205.0710 [hep-th]].
 - [43] S. Garcia-Saenz and S. Renaux-Petel, “Flattened non-Gaussianities from the effective field theory of inflation with imaginary speed of sound,” *JCAP* **11**, 005 (2018) doi:10.1088/1475-7516/2018/11/005 [arXiv:1805.12563 [hep-th]].
 - [44] J. Garcia-Bellido and D. Wands, “Metric perturbations in two field inflation,” *Phys. Rev. D* **53**, 5437-5445 (1996) doi:10.1103/PhysRevD.53.5437 [arXiv:astro-ph/9511029 [astro-ph]].
 - [45] D. Wands, K. A. Malik, D. H. Lyth and A. R. Liddle, “A New approach to the evolution of cosmological perturbations on large scales,” *Phys. Rev. D* **62**, 043527 (2000) doi:10.1103/PhysRevD.62.043527 [arXiv:astro-ph/0003278 [astro-ph]].
 - [46] F. Finelli and R. H. Brandenberger, “Parametric amplification of metric fluctuations during reheating in two field models,” *Phys. Rev. D* **62**, 083502 (2000) doi:10.1103/PhysRevD.62.083502 [arXiv:hep-ph/0003172 [hep-ph]].
 - [47] Y. B. Zel’dovich and I. D. Novikov, “The Hypothesis of Cores Retarded during Expansion and the Hot Cosmological Model,” *Soviet Astron. AJ (Engl. Transl.)*, **10**, 602 (1967)
 - [48] S. Hawking, “Gravitationally collapsed objects of very low mass,” *Mon. Not. Roy. Astron. Soc.* **152**, 75 (1971) doi:10.1093/mnras/152.1.75
 - [49] B. J. Carr and S. W. Hawking, “Black holes in the early Universe,” *Mon. Not. Roy. Astron. Soc.* **168**, 399-415 (1974) doi:10.1093/mnras/168.2.399

- [50] B. J. Carr, “The Primordial black hole mass spectrum,” *Astrophys. J.* **201**, 1-19 (1975) doi:10.1086/153853
- [51] G. F. Chapline, “Cosmological effects of primordial black holes,” *Nature* **253**, no.5489, 251-252 (1975) doi:10.1038/253251a0
- [52] B. J. Carr and M. J. Rees, “Can pregalactic objects generate galaxies?,” *Mon. Not. Roy. Astron. Soc.* **206**, 801–818 (1984) doi: 10.1093/mnras/206.4.801
- [53] J. Fumagalli, S. Renaux-Petel, J. W. Ronayne and L. T. Witkowski, “Turning in the landscape: A new mechanism for generating primordial black holes,” *Phys. Lett. B* **841**, 137921 (2023) doi:10.1016/j.physletb.2023.137921 [arXiv:2004.08369 [hep-th]].
- [54] T. Bjorkmo, R. Z. Ferreira and M. C. D. Marsh, “Mild Non-Gaussianities under Perturbative Control from Rapid-Turn Inflation Models,” *JCAP* **12**, 036 (2019) doi:10.1088/1475-7516/2019/12/036 [arXiv:1908.11316 [hep-th]].
- [55] G. A. Palma, S. Sypsas and C. Zenteno, “Seeding primordial black holes in multifield inflation,” *Phys. Rev. Lett.* **125**, no.12, 121301 (2020) doi:10.1103/PhysRevLett.125.121301 [arXiv:2004.06106 [astro-ph.CO]].
- [56] B. J. Carr, K. Kohri, Y. Sendouda and J. Yokoyama, “New cosmological constraints on primordial black holes,” *Phys. Rev. D* **81**, 104019 (2010) doi:10.1103/PhysRevD.81.104019 [arXiv:0912.5297 [astro-ph.CO]].
- [57] W. H. Press and P. Schechter, “Formation of galaxies and clusters of galaxies by selfsimilar gravitational condensation,” *Astrophys. J.* **187**, 425-438 (1974) doi:10.1086/152650
- [58] T. Harada, C. M. Yoo and K. Kohri, “Threshold of primordial black hole formation,” *Phys. Rev. D* **88**, no.8, 084051 (2013) [erratum: *Phys. Rev. D* **89**, no.2, 029903 (2014)] doi:10.1103/PhysRevD.88.084051 [arXiv:1309.4201 [astro-ph.CO]].
- [59] S. Young, C. T. Byrnes and M. Sasaki, “Calculating the mass fraction of primordial black holes,” *JCAP* **07**, 045 (2014) doi:10.1088/1475-7516/2014/07/045 [arXiv:1405.7023 [gr-qc]].
- [60] M. Sasaki, T. Suyama, T. Tanaka and S. Yokoyama, “Primordial black holes—perspectives in gravitational wave astronomy,” *Class. Quant. Grav.* **35**, no.6, 063001 (2018) doi:10.1088/1361-6382/aaa7b4 [arXiv:1801.05235 [astro-ph.CO]].
- [61] H. Niikura, M. Takada, N. Yasuda, R. H. Lupton, T. Sumi, S. More, T. Kurita, S. Sugiyama, A. More and M. Oguri, *et al.* “Microlensing constraints on primordial black holes with Subaru/HSC Andromeda observations,” *Nature Astron.* **3**, no.6, 524-534 (2019) doi:10.1038/s41550-019-0723-1 [arXiv:1701.02151 [astro-ph.CO]].
- [62] K. Ando, K. Inomata and M. Kawasaki, “Primordial black holes and uncertainties in the choice of the window function,” *Phys. Rev. D* **97**, no.10, 103528 (2018) doi:10.1103/PhysRevD.97.103528 [arXiv:1802.06393 [astro-ph.CO]].
- [63] S. Young, “The primordial black hole formation criterion re-examined: Parametrisation, timing and the choice of window function,” *Int. J. Mod. Phys. D* **29**, no.02, 2030002 (2019) doi:10.1142/S0218271820300025 [arXiv:1905.01230 [astro-ph.CO]].